SOL-GEL ENTRAPMENT AND SCREENING OF BACTERIA

THE ENTRAPMENT OF E. COLI IN SOL-GEL-DERIVED SILICA

FOR

COMPOUND SCREENING

By

NIKOLAS MENESES ELEFTHERIOU, B.Sc. (Honours)

A Thesis

Submitted to the School of Graduate Studies

in Partial Fulfilment of the Requirements

for the Degree

Master of Science

McMaster University

MASTER OF SCIENCE (2010) McMaster University

(Chemistry and Chemical Biology) Hamilton, Ontario

TITLE: The Entrapment of *E. coli* in Sol-Gel-Derived Silica for Compound Screening

AUTHOR: Nikolas Meneses Eleftheriou, B.Sc. (Honours) (McMaster University)

SUPERVISOR: John D. Brennan

NUMBER OF PAGES: ix, 71

Abstract

Sol-gel derived silica provides a bio-compatible material for the solid-phase entrapment of viable cells. A selection of *E. coli* cells containing unique promoter-linked GFP expression vectors were applied to fluorescence microwell plate assays, plate counting and various microscopy methods to assess changes in the entrapped bacteria and compatibility towards compound screening. Materials screening showed that a fast-gelation sol-gel composition from sodium silicate precursor and PBS buffer provided a consistently greater fluorescence signal than non-entrapped cells. It is shown for the first time that entrapped cells are capable of dividing within pockets of the silica gel, and can divide at a comparable rate to free cells. The entrapment of cells within a silica matrix does not induce the basal expression level of promoters tested here. Silica entrapment provides improved storage capabilities over non-entrapped cells in solution. A set of 12 related GFP-linked promoters were induced in solution and within silica when screened by two DNA gyrase inhibitors, providing similar expression profiles but greater signal-to-noise ratios in silica. The sol-gel derived material is amenable in an array format, and is a prospective material for the fabrication of sol-gel cell microarrays.

Acknowledgements

I thank John D. Brennan, the past and present members of the Brennan research group, the faculty and staff of McMaster University, and Regina Meneses for their kind support. Thanks to Julia Kolesnik for her assistance in performing part of the experimental work described in this document.

Table of Contents

List of Figures and Tables

List of Abbreviations

CFM – confocal fluorescence microscopy

CFMS – continuous-flow microspotter

CFU – colony forming units

DGS – diglyceryl-silane-derived sol

GLS – N-(3-triethoxysilylpropyl) gluconamide

GFP – green fluorescent protein

GPCR – G protein-coupled receptor

HTS – high-throughput screening

IPTG – isopropyl-β-D-thiogalactopyranoside

LB – Luria Bertani

MTMS - methyltrimethoxysilane

NAL – naladixic acid

NMR – nuclear magnetic resonance

NOR – norfloxacin

PBS – phosphate-buffered silane

PEG – poly-ehtylene glycol

PSMA – poly(styrene-co-maleic anhydride)

SEM – scanning electron microscopy

SiNa – sodium-silicate-derived sol

RNAi – RNA interference

TCM – transfected-cell microarray

TEOS – tetraethylorthosilicate

TMOS - tetramethylorthosilicate

Chapter 1 | Introduction

1.1 High-Throughput Screening and Microarrays

Small molecules are finding more use because they can probe or modulate biological systems. As the number of small molecules available is large, determining which small molecule will perturb each function becomes daunting without increased throughput. This is the basis for high throughput screening (HTS), in which many small molecules are assayed at once to determine which are acting on a desired target. The advantages of HTS include: i) improved efficiency compared to running many single assays, ii) very low volume requirements with a high number of assays in high-density microwell plates, ultimately conserving reagents and reducing time, and iii) automation.

HTS can be performed *in vitro*, or outside of a living organism by screening with an isolated protein, referred to as reverse genetics; or *in vivo,* inside a living organism such as cells or tissues, in which a phenotype is screened for, also referred to as forward genetics. Cell-based screening can be both advantageous and disadvantageous; the screen is successful if a probe for a specific phenotype is found (generating a "hit"); however the mode of action is often unknown. Protein-based screens will implicitly have a known mode of action through the nature of the assay; however the small molecules that have generated hits may be cytotoxic or may not be cell permeable in secondary screens.

Microarrays exist as a unique screening format since their introduction in the 1990's,[1-3] and are well established as a method for extreme miniaturization of a variety of *in vitro* assays (small molecule, protein, DNA).[4-6] Printing spots of nanoliter volumes of reagents onto glass slides, or alternative substrates, produces array elements in the 100 μm range that are ideal for reduced reagent and target consumption. Thus, the idea of a transition to cell-based microarrays becomes appealing, and current cell-based microarray methods have proven useful for a variety of assays including, but not limited to, detecting enzyme activity, signal transduction, transcription levels and response to external stimuli.[7-9]

Examining current cell-based microarray formats shows various novel methods for immobilizing cells onto microarrays, however some key problems suggest room for improvement. Mainly, there is a lack of a robust screening platform which allows for facile, multidrug versus multi-target assessment with drop-on-demand microarray printers. The following outlines current cell microarray technologies, followed by an introduction to sol-gel chemistry as a method for cell entrapment, culminating in how sol-gel materials are can be applied to the fabrication of multiplexed cell microarrays utilising reporter-gene-linked cell arrays.

1.2 Current Technologies for Fabricating Cell Microarrays

Of the many methods for fabricating cell-based microarrays via robotic printing, the methods of particular interest are those that allow the spatial separation of unique pre-determined cell types, made possible through the use of various immobilization

techniques. This should allow the microarray to become immersed in liquid, or cultured onto a microbial plate. Cell-based microarray methods have been developed that improve the spatial distribution of cell targets by isolating unique array elements, and is described in further detail below.

Microarrays have been prepared through the attachment of cell-surface recognition sequences to specific capture agents such as peptides, small molecules, DNA ligands, histocompatibility complex proteins or extra-cellular matrix components,[9-11] immobilizing the cell through its external surface features. However the use of capture agents requires high specificity and selectivity for the membrane-bound targets in order to limit interferences and false positives. Detectable cell features for capture agents are limited to the extracellular matrix, and as such, these methods fail to be broadly applicable when working with a single strain containing unique mutations or plasmids. High background signal may also be problematic if there is cell adhesion onto blank regions, as may be the case with adherent mammalian cell lines.

Some high-density microarray platforms have been presented by printing unique bacterial or yeast cell lines onto molecule-permeable membranes creating nanocraters (Figure 1.1).[12] These methods allow for the cells to form colonies directly or indirectly over a solid nutrient support containing the drug of interest; this allows for the analysis of many cell lines, but are limited in throughput as they are not amenable to liquid handling

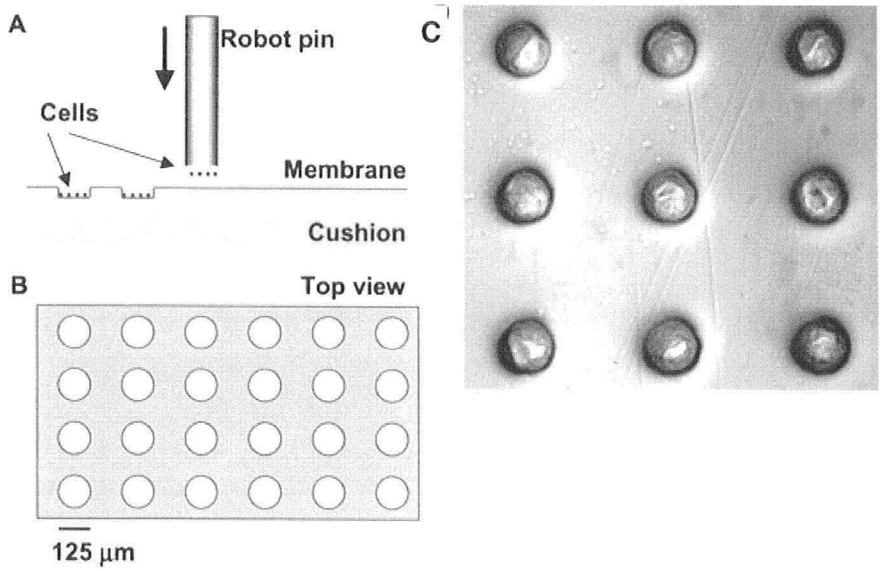

Figure 1.1 Schematic for fabrication of nanocrater cell microarrays. (*A*) Robotic pin print cells onto a cellulose ester membrane to form nanocraters and simultaneously inoculate cells into them. (*B*) Top view of arrayed nanocraters. The diameter of the nanocraters was 125 μm, and the distance between centers of the adjacent nanocraters was 375 μm. *(C)* Nanocraters with yeast cells at their bottoms (Adapted from Xu *et al.* 2002, Ref # 12).

robotics and multicompound screening. Nanocrater arrays are limited to cells that are grown on compatible solid media. The cell samples are printed on top of the hydrogel and are not immobilized, allowing cross-contamination between array elements once immersed in a liquid media.

Other microarray methods directed at mammalian cell lines are largely dependent on the adhesive monolayers that form when cultured. In particular, transfected-cell microarrays (TCMs, Figure 1.2)[13] involve a printed array of hydrogels containing unique expression vectors, each vector encoding for distinct cDNAs, protein overexpression, or RNA interference (RNAi) sequences for gene knockdown.[14-17] A monolayer of mammalian cells is then seeded over top of the entire array, allowing gene

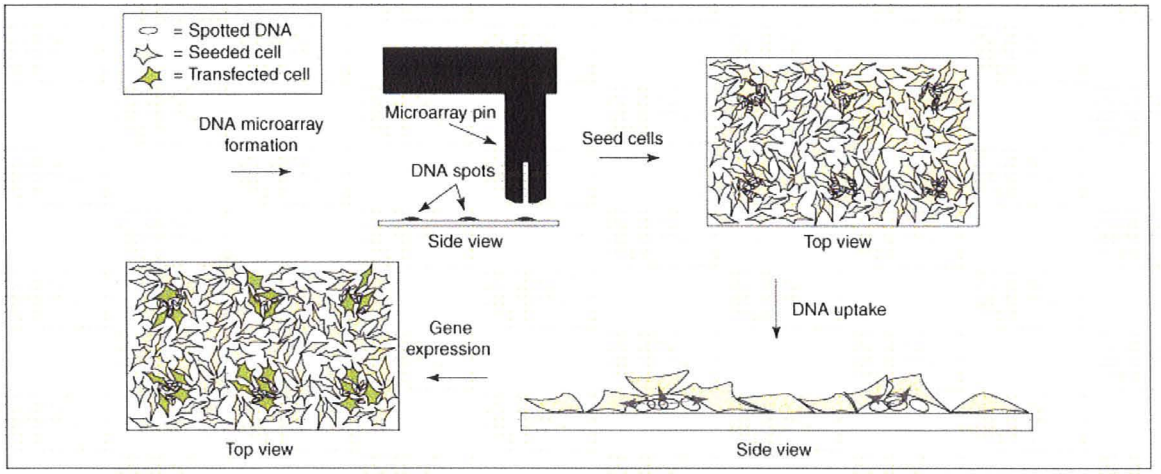

Figure 1.2 Schematic of the formation of a transfected-cell microarray. First, DNA is transferred to a solid surface using a robotic spotter for the formation of a DNA microarray. Second, cells are seeded and attach to the surface to form a lawn of cells on top of the DNA microarray. Third, DNA is released from the surface and only taken up by cells that attach to regions where DNA is present (grey arrows indicate the movement of DNA). Fourth, transfected cells express the genetic information represented by the uptaken DNA. (Adapted from Hook *et al.* 2006, Ref #13).

delivery and expression only by local cells. With many applications, TCMs have been effective in: recognizing proteins involved in kinase signaling,[14] apoptosis,[16] cell-cell adhesion,[18] and GPCR interactions,[19] a mammalian two-hybrid screening method has been employed;[20] and high-content readouts of subcellular phenotypes and cell morphology have been demonstrated.[21] Mishina *et al.* have also shown that TCMs can be arrayed within microwell plates and made compatible with liquid handling robotics for compound screening.[19]

TCMs are dependent on the adhesive properties and characteristic monolayer of mammalian cells. Several advancements have been made to improve cell adhesion through substrate modification: model immortal cancer (HeLa) cells have shown

improved adhesion on collagen chitosan-modified surfaces;[22] likewise model neuroblastoma (SK-N-SH) and human embryonic kidney (HEK 293) cell adhesion improves with phenylazide modified polymers on poly(ethyl glycol) treated slides which exhibit low background adhesion.[23] Although the use of TCMs has been extensive, this format is unsuited for cells that readily translocate into a liquid suspension, for instance blood cells, bacteria and yeast, reducing control over cross contamination. Furthermore, TCMs are not compatible with screening multiple strains or cell lines in a single array, otherwise, seeding mixed cell lines would result in incoherent readouts from individual spots.

Finally, the efficiency of solid-phase transfection for some cell lines can be considerably reduced compared to the liquid phase, making TCMs unreliable for these assays.[16] Poor transfection has been improved in some cell lines through the application of lentiviral infections that can transfect a larger breadth of mammalian cells, but does not offer a universal solution and requires high concentrations of the lentiviral vectors.[24] TCMs are also compatible with electroporation for gene delivery,[25] but require specialized equipment that may not be amenable to a HTS scale.

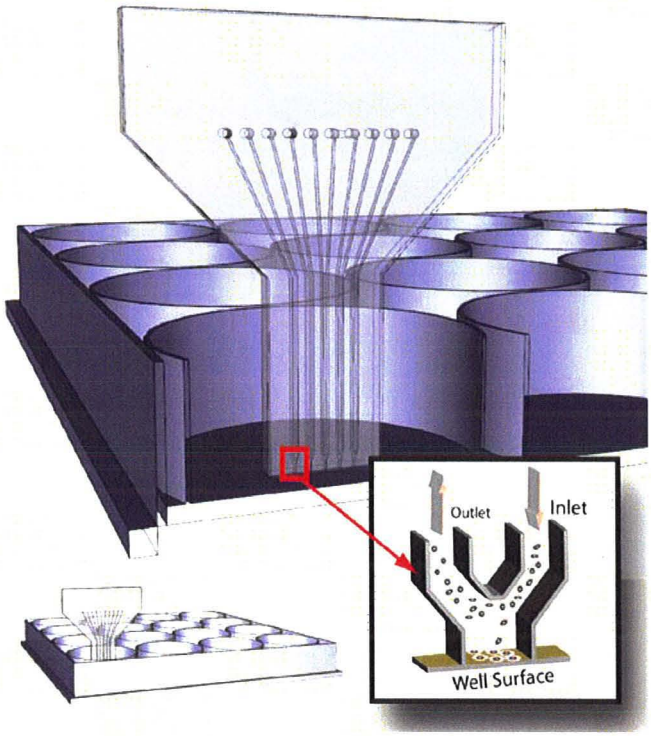

Figure 1.3 Overview of the microfluidic cell patterning device. The continuous flow microspotter is shown contacting the well bottom (16 mm diameter). Parallel sets of microchannels run perpendicular to the well bottom. The area of the well surface isolated by the deposition chamber is 200 μm×300 μm to pattern a proportionate cellular microspot. (Adapted from Sincic *et al.* 2009, Ref # 26).

The methods described thus far utilize currently available robotic pin-printing instruments to fabricate cell microarrays. *Sinic et al.* describe an alternative approach to patterning microarrays of unique cell lines with a custom microfluidics device compatible with microwell plates.[26] The continuous flow microspotter (CFMS) head was designed with inlet and outlet microchannel pairs that run perpendicular to the surface of a microwell plate, where each pair of inlet and outlet channels can deposit unique adherent

cell lines to the microwell bottom (Figure 1.3). The study demonstrates the application of five parallel experiments with wild type or mutated Chinese hamster ovarian (CHO) cells within one well, each with a surface area 300 x 200 μm, but suggest that a multilayer CFMS can print up to 48.

New custom-designed microfluidic tools such as the CFMS are appealing because they have the potential to fabricate multiplexed cell arrays amenable to HTS liquid handling robotics similar to pin-printing methods, but have the advantage of being highly programmable, (i.e. variable flow rate, deposition pattern, etc.). However, contact and non-contact array printers are widely available commercial devices capable of much higher density arrays; the demonstrated density of one CFMS array was only five samples in one 16 mm-diameter well. The CFMS is also dependent on the adherent properties of some cell lines. While the invention of new instrumentation for cell microarrays can address some of the problems discussed with current methods, it may be more economical to use existing printing technologies while exploring materials chemistry.

The methods for cell microarray fabrication described thus far have focused on binding: cell adhesion, surface attachment, and printing onto solid nutrient gels. Entrapment of cells is another approach for active immobilization, and with the use of porous polymers, has been widely studied for the development of biocatalysts and bioreactors.[27-29] Within the past six years there have been developments in the use of

alginate encapsulation in cell microarrays, for bacterial and yeast,[30] and mammalian cell lines.[31-33]

Alginic acid is an unbranched polysaccharide extracted from seaweed consisting of mannuronate and guluronate residues. The polymer undergoes an ionic-exchange gelation upon the addition of a divalent cation (typically Ca^{2+} and Ba^{2+}) to alginate in solution, described by an egg-box model in which co-operative binding of a divalent cation with the polyguluronate residues form a chelated structure, (much like eggs in their packaging).[34,35] This characteristic of alginate allows for selective control of gelation by adding divalent cations and chelating agents to the alginate-cell mixture; barium is preferable to calcium since calcium is implicated in various signaling pathways.

In applications of alginate for cell microarrays, the biocompatible hydrogel-cell mixture is printed in an array and is allowed to undergo gelation on a microchip before being immersed in media (Figure 1.4). Early work has shown that i) alginate gels can entrap cells on microarrays, ii) cells are able to grow within these array elements, and iii) GFP fluorescence and live-cell staining are both quantifiable using fluorescence microscopy.[30] However, alginate gels must be printed onto treated surfaces, such as with poly(styrene-co-maleic anhydride) (PSMA) or methyltrimethoxysilane (MTMS),[31,36] in

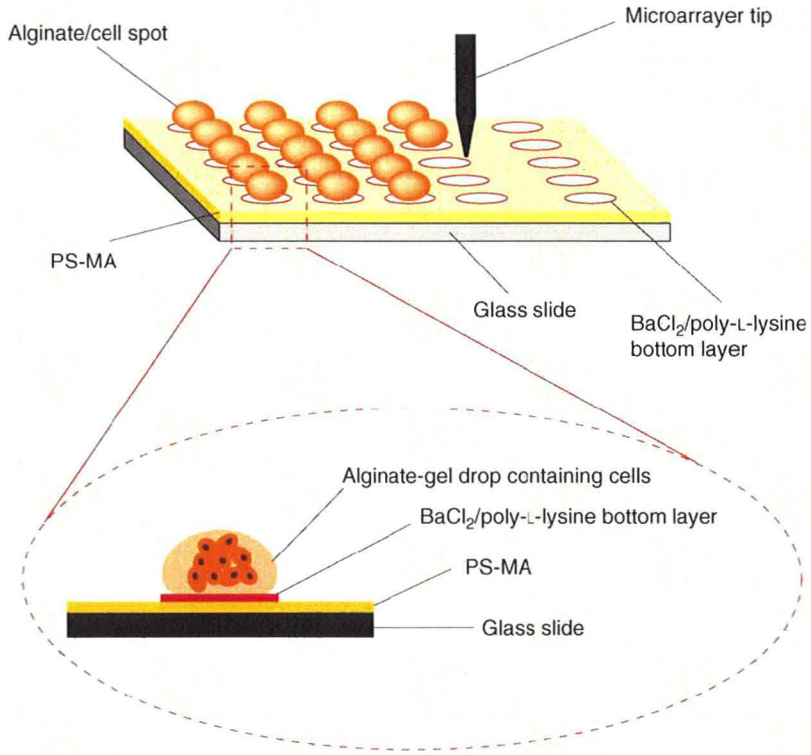

Figure 1.4 Schematic illustration of a high-throughput 3D cellular microarray platform. Cells are directly spotted on functionalized glass slides using a microarray spotter. Cell encapsulation is the result of alginate gelation mediated by the presence of Ba^{2+} ions. Positively charged poly-L-lysine promotes attachment of the negatively charged polysaccharide constituent of alginate upon gelation, keeping each spot in its location. PS-MA: poly(styrene-co-maleic anhydride). (Adapted from Fernandes *et al.* 2009, Ref # 32).

order to improve attachment of the hydrogel matrix, and have not been reported in microwell plates.

While the alginate hydrogels provide a readily available and biocompatible method of entrapment, its use is also dependant on the constant presence of calcium or barium ions despite possible biological interferences. Alginate gels are have poor

chemical inertness, as they are incompatible with phosphate buffers, due to phosphate chelation,[37] as well as other chelating agents, and the mechanical strength of organic polymers are much weaker than a silica matrix.[38 39]

1.3 Sol-Gel Process

The entrapment of cells through the polycondensation of silica sols presents itself as an alternative to alginate hydrogels. The bio-applications of sol-gel materials are broad; proteins, nucleic acids, antibodies and whole cells can all be successfully encapsulated into silica matrices.[40] The Brennan group has extensively studied sol-gel methods in order to entrap a variety of biologicals and develop solid-phase assays, including protein microarrays using sol-gel derived silica.[41-44] Furthermore, many cell types have been successfully been trapped within sol-gel matrices, including various bacterial,[45-47] yeast,[48-50] animal,[51,52] vegetal[49,53,54] and algal cells.[55] Bioencapsulation typically requires two steps to form a silica matrix, (Figure 1.5). The first step is to produce a precursor sol, often from the hydrolysis of various silanes; the next step is to mix the sol with a buffered biological sample to induce polymerization. The most common sols in practice are produced from alkoxide, aqueous or sugar-based precursors: alkoxide silicates such as tetramehtylorthosilicate (TMOS) and tetraethylorthosilicate (TEOS) are hydrolyzed with hydrochloric acid, and will release methanol and ethanol, respectively; diglycerylsilane (DGS) undergoes hydrolysis in water and releases glycerol,

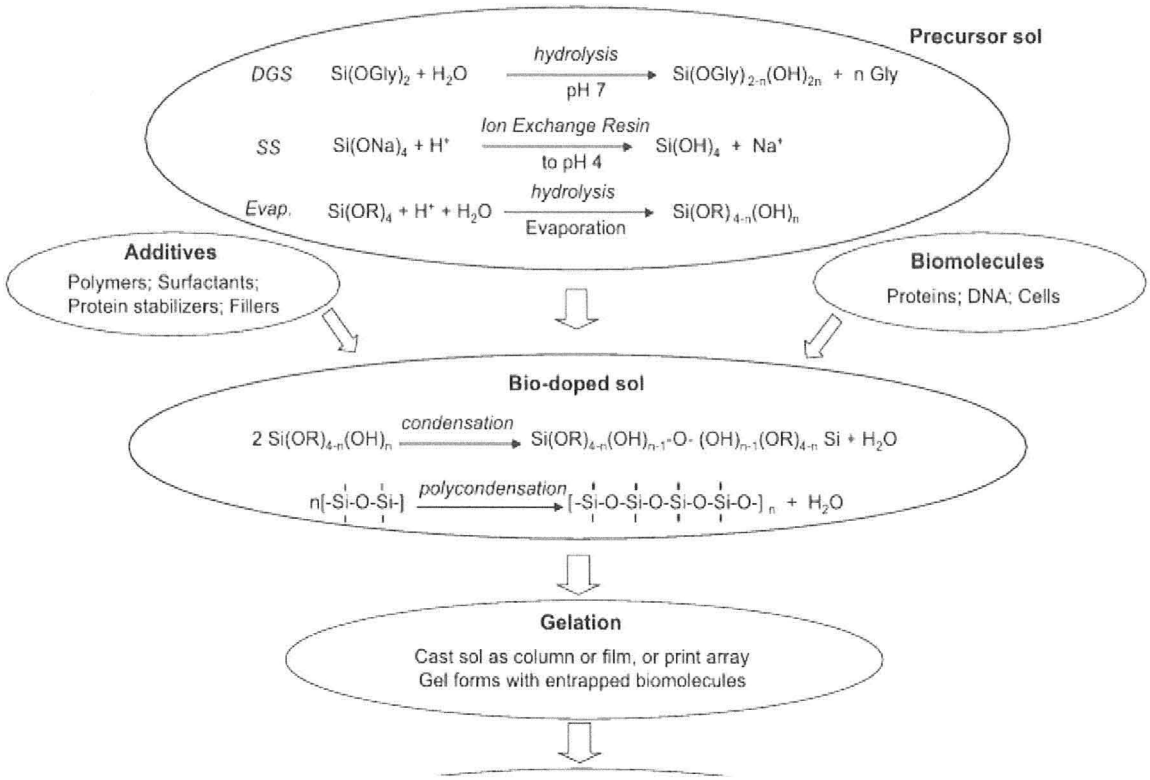

Figure 1.5 Schemes for fabrication of sol-gel materials. (Adapted from Brennan *et al.* 2007, Ref # 61).

a protein stabilizer,[56] but is not commercially available; sodium silicate solutions are mixed with a cation-exchange resin to remove sodium ions and replaces them with hydronium ions.[57,58]

Gelation is promoted once the ionic strength of the sample is increased, such as by the addition of a buffered biological sample, neutralizing low pH conditions by the sol. The sol-gel process is practical for entrapment of biologicals for several key reasons: the necessary reactions are performed without exposing the sample to high-temperatures or extreme pH conditions;[59] the resulting silica matrix can be adjusted through pore size and gelation time by varying the pH buffer and the inclusion of various

additives if desired;[41,60] the gelation process is compatible with many buffer types; the silica matrix is porous enough to allow small molecules to pass through while keeping larger biologicals entrapped;[61] and the silica matrix is compatible with many simple and complex spectroscopic analytical techniques.[62,63]

1.4 Sol-Gel Encapsulation of Cells

The application of sol-gel materials for the encapsulation of active cells was first reported by Carturan *et al.* in 1989.[64] *Saccharomyces cerevisiae* (yeast) were successfully entrapped within thin films deposited on glass substrates. Yeast was first entrapped since it can withstand harsh conditions including the release of alcohols from alkoxysilane sol precursors. The successful encapsulation of cells has made sol-gel materials an appealing option for the fabrication of biosensors[65,66] and bioreactors.[47,67-69]

Sol-gel chemistry has also inspired more sophisticated methods of entrapment, demonstrated by the encapsulation of various mammalian cells using the Biosil process,[51] in which gas-phase alkoxysilane precursors pass over wet cells until the precursor reacts with available water and forms a surface-conforming silica scaffold overtop (Figure 1.6). Entrapped cells have since been shown to remain metabolically active upon entrapment,[51] and there has been progress in developing this technology for bio-artificial organs and cell-grafting.[70,71] In one example, Biosil-encapsulated pancreatic islets transplanted into diabetic rats have been shown to reduce glycemia through the production of insulin.[72]

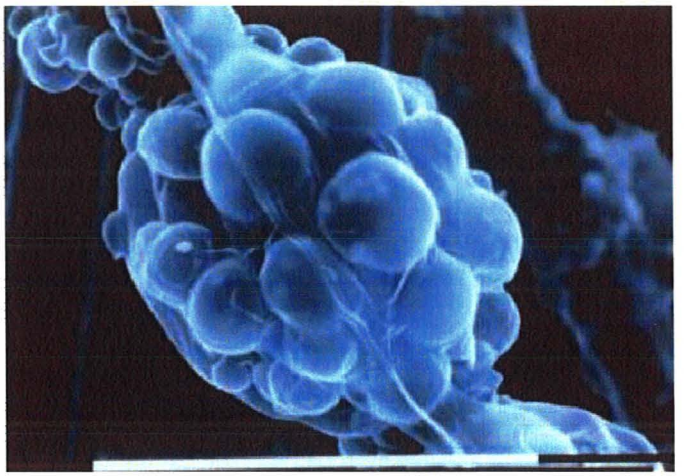

Figure 1.6 Human fibroblasts on glass fibres and coated by the Biosil process. (Adapted from Carturan *et al.* 1998, Ref # 54).

The development towards biosensors, bioreactors and bio-artificial organs demonstrate the versatility of silica matrices for cell encapsulation. However, these applications exploit a specific feature of the encapsulated cell, such as the response to external stimuli or metabolite turnover. Although encapsulated cells are in a defined chemical environment, it is certainly not the native environment for species under investigation, and although the silica matrix is biologically inert, it remains unknown how entrapment within a shrinking matrix affects the cell physiology and gene regulation.

However, there have been contributions made towards evaluating cell physiology through stress response and cell viability of encapsulated bacterial cells. *Escherichia coli* cells were often selected as a model bacterial system since they have a fast division time and are easily genetically engineered. The first reported encapsulation of *E. coli* shows that cells are randomly dispersed within TMOS-derived silica matrix, and that enzymatic activity is retained within wet gels despite the presence of methanol.[45] Soon after, it was

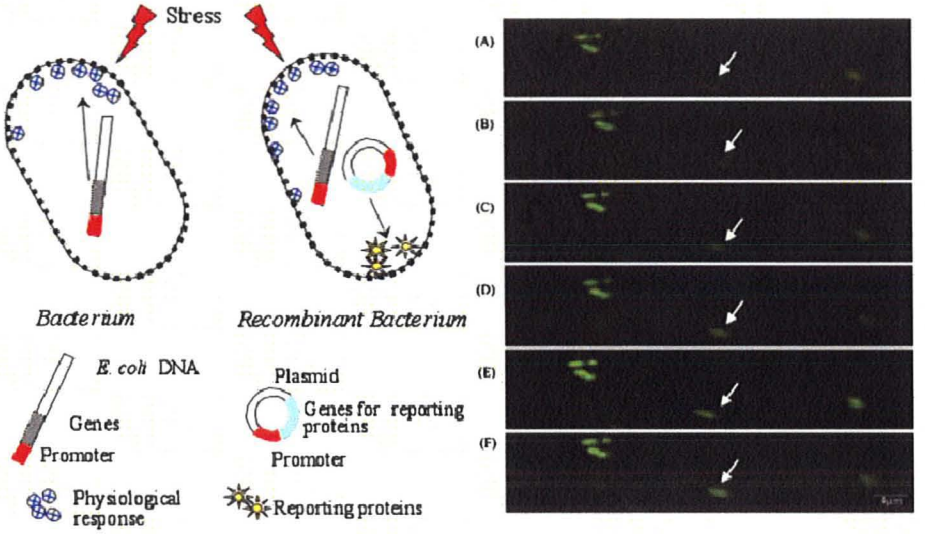

Figure 1.7 Left: stress induced response of native and recombinant bacteria. The recombinant bacterium expresses reporting proteins in addition to the physiological defense mechanism of the native bacterium. Right: single E. coli cell fluorescent response after induction by 1.2 mmolar mitomycin C. Confocal microscope images were taken after incubation times of 0, 140, 260, 340, 420, and 480 min. (Avnir *et al.* 2006, Ref # 40).

shown that aqueous silica routes for entrapment using sodium silicate is less harmful towards cell viability and enzymatic activity, compared to alkoxide silicates.[73]

Premkumar *et al.* confirmed using confocal fluorescence microscopy of fluorescent GFP-expressing *E. coli* that there was no visible cell growth within the porous silica matrices, an idea which has since been maintained, and that molecular oxygen is accessible to cells deep within the silica gel (as it is required for GFP fluorescence).[74] The effects of stress upon entrapment were investigated using fluorescence and luminescence reporters for heat shock, oxidative stress, fatty acid availability, peroxides and genotoxicity, all of which showed similar behaviour when induced in solution and in silica, and showed no background levels indicative of stress as a direct result of entrapment in TMOS-derived matrices (Figure 1.7).[46,74]

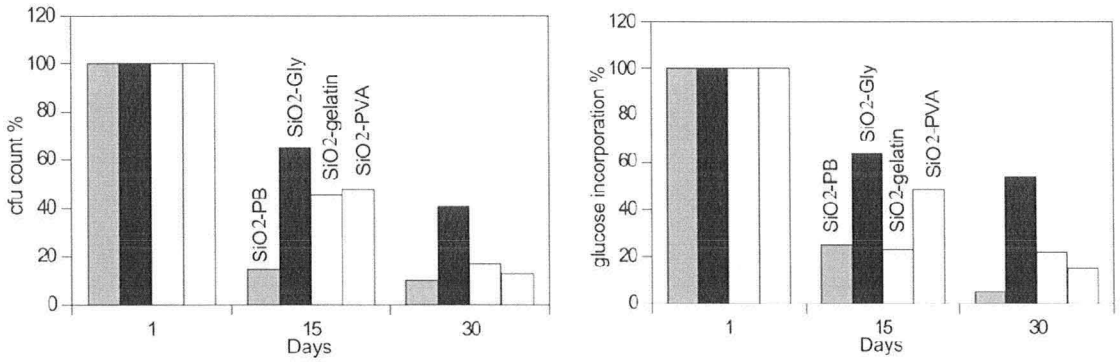

Figure 1.8 Left: Evolution of colony formation unit (cfu) count of entrapped cells in the four gels aged one, fifteen and thirty days. The error range is within 20–30%. Right: Evolution of [^{14}C]glucose incorporation in entrapped cells in the four gels aged one, fifteen and thirty days. The error range is within 20–30%. (Adapted from Nassif *et al.* 2003, Ref # 75).

Cell viability, often determined by the number of colony forming units (CFU) from crushed gels suspended in saline solution, could be maintained from several months to one-and-a-half years depending on the matrix composition.[46, 75] Silica gels containing glycerol further improved viability determined using [^{14}C]glucose incorporation methods as well as CFU determination, where the fraction of detectable [^{14}C]glucose incorporation was homologous to the fraction of CFU from gels containing entrapped cells stored for, and then crushed, after 15 and 30 days (Figure 1.8). This was supported by differences in glucose metabolism for glycerol-containing and glycerol-free gels determined by ^{13}C NMR, where glycerol-containing samples had shown lower concentrations of un-metabolized glucose over one month indicating conditions in which glucose metabolism is better supported.[76] While glycerol improves viability for some months, a 550-day test showed complete cell death compared to samples containing no added glycerol or additives with exception of saline solution.[75] Furthermore, there are no significant

differences reported in the viability of bacteria entrapped while in growth phase or stationary phase.[75] The research surrounding the silica entrapment of cells, in particular the model bacterium *E. coli,* has shown cells can remain viable within the silica matrix while appropriately responding to external stressors, that the matrix has not induced any of the stress response genes previously tested, and that the cells can be entrapped within a variety of modified silica matrices with good structural integrity. The cell-compatible silica materials are a new target for chemical screening of cells and should be assessed for cell microarrays.

1.5 Sol-Gel Chemistry for Cell Microarrays

Sol-gel materials provide an appealing alternative for the development of bacterial cell microarrays given the previous research above. Sol-gel chemistry allows the facile extension of any microarray platforms developed since sol-gel entrapment is not specific to the innate properties of the species being entrapped; *i.e.* it is applicable to non-bacterial cells. Furthermore, sol-gel derived microarrays have been fabricated for the study of proteins,[42, 44, 77, 78] and materials optimization can be completed in high throughput for signal optimization and viability of cells.[79]

The printing of microarrays is traditionally performed with either contact or non-contact printing methods. Contact pin-printing has previously been applied to printing sol-gel-based protein microarrays with success, but has limitations in the materials that can be printed.[79] Wonton *et al.* describe printing a set of compatible sol-gel derived materials that produced highly active protein array elements.[79] However pin-printing

methods for sol-gel materials impose several limitations, the main requirement being a long gelation time for the sol-buffer mixture to be printed so that gelation does not occur within the pin.

Preliminary studies on cell microarrays using sol-gel encapsulation were produced by Xin Ge and John Brennan (unpublished). Arrays were successfully fabricated from aqueous sols mixed with glycerol and buffered *E. coli* cells printed onto untreated glass-bottom microwell plates; *E. coli* strains carried inducible promoters for *gfp* expression (Table 1.1). High-density sol-gel derived cell microarrays showed improved signal induction compared to alginate based arrays (Figure 1.9). Most importantly, multiple cell strains were shown to be selectively induced and repressed within a single microarray (Figure 1.10). These early results demonstrate the capability for highly multiplexed arrays with low reagent consumption.

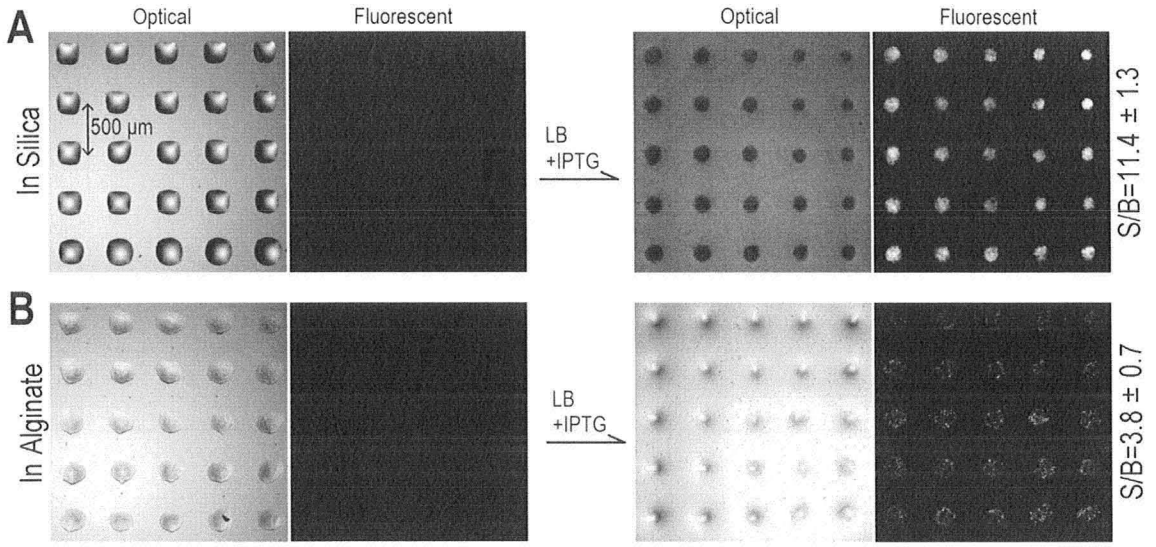

Figure 1.9 Viability of cell microarrays demonstrated by reporter gene expression. *E. coli* stain BL21 (DE3) pLys, carraying plasmid pET23a-eGFP, was immobilized in sol-gel based silica (A) and alginate (B) materials. Both optical and fluorescent images were obtained for arrays either before or after incubation in LB media without (left) or with (right) 1 mM IPTG. Signal to background ratios (S/B) are listed besides of images. (Adapted from Ge, X. and Brennan, J.D., 2008, unpublished)

Table 1.1 Bacterial strains and plasmids used. "+" and "-" refer to induction (+) or suppression (-) of the promoter.

Plasmid	*E. coli* Strain	Promoter	Regulators used	GFP variant	Excitation maximum
pET23a-eGFP (gift from Dr. G. Wright, backbone from Novagen)	BL21(DE3)pLys (Novagen)	T7	+IPTG	eGFP	488 nm
pGLO (Bio-Rad)	HB101 (Bio-Rad)	*araC*	+arabinose; -glucose	GFPuv	370 nm

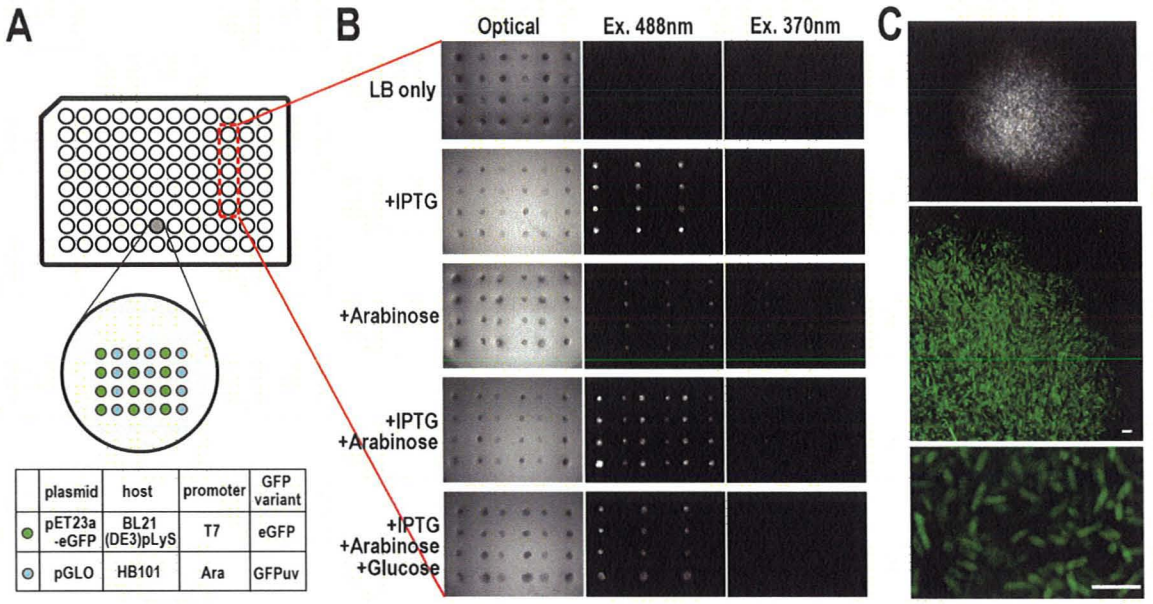

Figure 1.10 Multiplexed assays using cell microarrays. (A) Diagram demonstrating the pattern in which cell microarrays were super-gridded into a 96-well plate (top). In each single well, two cell strains were pin-printed in alternate columns (middle). Information on the two E coli strains, including plasmid, host cell, promoter, inducer, and GFP variant, are listed (bottom). (B) Images of 5 cell microarrays separately located in 5 wells of a microplate, after incubation in 5 different culture media (LB only; with addition of IPTG; arabinose; IPTG and arabinose; IPTG, arabinose and glucose). Three images were taken for each cell array – an optical image, and fluorescent images excited at 488 nm and 370 nm. (C) Microscopic images of an individual microspot in the array (top), a higher magnification image of part of a spot (middle), and a high magnification image of individual *E coli* cells immobilized in silica gel (bottom). Scale bars are 5 μm. (Adapted from Ge, X. and Brennan, J.D., 2008, unpublished)

This thesis project previously focused on developing sol-gel cell microarrays, but encountered significant problems with contact-pin printing in the development of these assays. The highlights of these problems are: optimal material development was limited to those that have long gelation times as to not undergo gelation before printing; and microarrays experience harsh post-gelation conditions, such as immersing them in growth media, and were not compatible with maintaining the structural integrity of the long-gelation-time array elements. These problems exaggerated the variability in day-to-day reproduction of sol-gel-based microarrays, resulting in impractical array elements. Non-contact printing methods may be favourable because the independent deposition of buffer and sol allows greater versatility in optimal materials. A fast gelation time is ideal since a high structural integrity is quickly reached, and the array elements remain hydrated until the addition of media. While non-contact array methods seem best suited for this, it is unknown what problems may exist when printing nanolitre array elements with new instrumentation.

1.6 Thesis Goals

The entrapment of bacteria has been applied to the development of bioreactors and biosensing platforms or prospects. These do not necessarily require that cells divide, but have been shown that they are not easily prone to stress and have long-term stability. The studies previously published regarding the sol-gel encapsulation of bacterial cells have been focused on the development of bioreactors or biosensors, and show that cells retain long-term viability, up to one-and-a-half years, and that the process of entrapment

does not instigate the expression of major stress genes, additionally there has been no evidence of cell division within the silica matrix. However, the research completed is far from comprehensive; it is indeterminate as to how all cell pathways behave upon entrapment. For instance, there may be changes in the regulation of genes that control the division of bacteria, cell-cell communication, or the extra-cellular surface content, each of which can be altered by the spatial restrictions for growth, the diffusion of metabolites through the porous matrix, or interaction with the partially-charged silica, respectively.

Considering that there are many unknown facets in the relationship between a silica matrix and the entrapped bacterial cells, the goals of this thesis are as follows: i) perform a material screen to find a highly cell-compatible matrix; ii) evaluate the matrix capabilities for cell growth; iii) vary the conditions of entrapment to assess ideal assay conditions and limitations of cell entrapment; iv) assess the activity of a set of promoters to describe changes to cell physiology upon entrapment; v) perform an induction assay with a set of promoters known to respond in solution; and vi) assess the printability of cell arrays with a sol-gel composition in sub-microliter volumes.

The long-term goal, beyond the scope of this thesis, is to fully develop a solid-phase cell microarray that allows for simultaneous multi-pathway screening of fluorescent bacterial cells. This HTS method will allow for rapid identification of small compound-promoter relationships. As facets of the effects of encapsulation on bacterial cells remain unknown, various microscopy methods, material screening and monitoring

of promoter expression levels were applied to develop a model for the behavior of cells within a silica matrix. These methods are selected to investigate the effects of sol-gel entrapment on bacterial cells, and to better understand whether these effects are beneficial or detrimental to the application of sol-gel solid phase assays for chemical screening. The fabrication of low-density sol-gel microarrays was also attempted with non-contact liquid handlers to assess the assay volume reduction and compatibility with the sol-gel materials.

Cell screening was made possible with the Alon collection of *E. coli* containing transcriptional fusions of *gfp* to around 2000 different promoters.[80] A selection of GFP-linked promoter strains of *E. coli* were selected that report on cell growth, cell division and the cell envelope; transition into stationary phase; and heat shock, osmotic stress, and general stress; and are predicted to potentially exhibit changes in expression levels as a result of entrapment, relative to solution. A second set of genes was selected that are expected to respond to quinolone DNA gyrase inhibitors, and were induced in solution and in silica to evaluate differences in expression response as a preliminary on a practical drug target. A practical criteria for the successful fabrication of a solid-phase cell array is to ensure that expression levels are conserved between assays in solution and in a silica matrix, making the method compatible with chemical and drug discovery screening.

Selection of a practical silica-hybrid material is also considered. The use of aqueous sols is favourable as it provides the release of water upon condensation, whereas

alkoxide routes release alcohols and can be harmful towards the entrapped cells. The manipulation of the silica matrix was done with modified silanes and additives, and is evaluated by the constitutive and high-expression rRNA promoter *rrnB*. Measurement of GFP-expression levels was determined with microwell plate readers in real-time and endpoint experiments. Sol-gel encapsulated cells were further characterized with cryogenic scanning electron microscopy (cryoSEM) to better observe the water distribution of the hydrogels, and confocal fluorescence microscopy (CFM) to observe bacteria for cell division.

Lastly, a promoter activity assay was reproduced with a non-contact pneumatic liquid handler, capable of pneumatically printing volumes in the 100 nL range in lieu of a non-contact piezoelectric microarray printer, which is capable of printing array elements on the sub-nanoliter scale.

Chapter 2 | Experimental

2.1 Materials

Sol precursors were sodium silicate solution (29.2% SiO_2, 9.1% NaO, 61.7% H_2O, Fisher Scientific), and diglyceryl silane synthesized in house as described elsewhere and validated with ^{29}Si NMR.[56] A DOWEX 50WX8 resin (Sigma-Aldrich) was used as the ion-exchange resin for preparation of sols from sodium silicate. LUDOX HS-40(Aldrich) was used as a source of colloidal silica. Additives were glycerol, poly(ethylene glycol) (PEG, typical Mn 1,000, Sigma-Aldrich), N-(3-triethoxysilylpropyl) gluconamide (GLS, 50% in EtOH, Gelest). Ethanol was evaporated off from GLS before use. All reagents were used without further purification.

Antibiotics used were kanamycin solution (Sigma), nalidixic acid (NAL, Sigm-Aldrich) and norfloxacin (NOR, Fluka). The following growth media and buffers were used: Luria-Bertani (LB) broth, LB agar (1.5% w/v agar in LB broth), 1X M9 minimal media, 1X phosphate-buffered saline (PBS, pH 7.5) and HEPES (87 mM, pH 7.5). 1X buffers and media were autoclaved before use. Cell staining was done with Gram's Crystal Violet Solution (Fluka) and Gram's Iodine Solution (Sigma-Aldrich) used as is; safranin O (2.5g, Sigma) was dissolved in 100 mL of 95% ethanol, and later diluted 10-fold in ddH_2O before use. ddH_2O was obtained from a Milli-Q Synthesis A10 system (Millipore, Billerica, MA).

2.2 Bacterial Strains and Growth Conditions

All media and buffers were supplemented with kanamycin to a final concentration of 25 μg/mL. LB-glycerol stocks of E. coli cultures were grown overnight in a shaking incubator at 37°C in LB broth. Cells were later subcultured at 2% v/v into M9 minimal media and grown to an OD_{600} of 0.2 before use, corresponding to the early exponential growth phase. Sterile technique was practiced throughout the handling of cell cultures.

A selection of *E. coli* K12 strain MG1655 cell lines were used from the Open Biosystems *E. coli* Promoters collection (Thermo Scientific). All cells contain a pUA66 plasmid encoding a *gfpmut2* gene; various *E. coli* K12 promoters are located upstream of the *gfpmut2* gene and will express GFP as a response to the native expression of the upstream promoter. The *rrnB* promoter, controlling the expression of 16S rRNA, was used as a constitutive high-expression cellular reporter,[80,81] and the strain containing the promoterless-plasmid pUA66 was used as a control for background fluorescence. The remaining selection of promoters is highlighted in Tables 2.1 and 2.2, for reporters to DNA gyrase inhibition and hypothetical reporters to sol-gel entrapment, respectively.

2.3 Sol-Gel Encapsulation

Sols were prepared as previously described elsewhere.[44,56] Briefly, sodium silicate sols (SiNa) were prepared by mixing 2.56 g sodium silicate solution, 10 mL ddH_2O and

Table 2.1 Promoters used to study the response to two DNA gyrase inhibitors. Promoter descriptions from *E. coli* Promoter Collection, The Weizmann Institute of Science.[80]

Promoter	Description
recN	protein used in recombination and DNA repair
sulA	inhibitor of cell division and FtsZ ring formation upon DNA damage/inhibition
recA	DNA strand exchange and recombination protein with protease and nuclease activity
lexA	transcriptional repressor for SOS response
rmuC	conserved protein
yfbM	conserved protein
yjbJ	unknown coding sequence
valV	valine tRNA
ybhE	putative isomerase
minC	cell division inhibitor; activated MinC inhibits FtsZ ring formation
osmE	transcriptiaonal activator of *ntrL* gene
nmpC	outer membrane porin protein

Table 2.2 Promoters used to study the cellular response to sol-gel entrapment. Promoter descriptions from E. coli Promoter Collection, The Weizmann Institute of Science and additional references.[80]

Promoter	Description	Additional References
rpoH	heat shock regulon induced by cytoplasmic stress	82
ompX	outer-membrane protein; implied in extreme pH response	83
pyrB	aspartate carbamoyltransferase; general stress response	84
cspD	DNA-binding protein; induced during stationary phase	85
rpoE	responds to periplasmic stress; detect and respond to changes in bacterial envelope; heat shock regulon	86
nlpI	lipoprotein involved in cell division	
ompR	transcriptional regulator affecting outer membrane protein synthesis	
otsB	trehalose-6-phosphate phophatase; induced during stationary phase and osmotic stress	87
envY	transcriptional activator of envelope proteins; thermoregulation of porin biosynthesis	
rpoD	major sigma factor during exponential growth	
rpoS	entry into stationary phase; responds to increase in osmolarity	88
dps	stress response; long-term survival of cells; pH response	85,83
mraZ	involved in formation of the cell envelope and cell division	
rpsL	30S ribosomal subunit protein	

4.5 g charged ion-exchange resin for 1 minute, vacuum filtered, and filtered through a 0.45 μm filter; the ion-exchange resin was charged with 0.1 N HCl, and then vacuum-filtered until dry. Diglyceryl silane sols (DGS) were prepared from diglyceryl silane crushed to a fine powder, added to water at concentrations of 0.25-0.5 g/mL, sonicated in ice water for 20 minutes with occasional mixing, and filtered through a 0.2 μm filter. Sols were stored on ice and used soon after preparation. Sols were added 1:1 (v:v) with buffer containing cells or additives. Cells were added at 1% v/v of total assay volume in sol-gel and solution experiments. Sols mixed with PBS and HEPES buffer underwent gelation after ten and forty minutes, respectively.

2.4 Microwell Plate Assays and Analysis

Promoter expression levels were determined using fluorescence measurements in NUNC and BD Falcon 96-well optical-bottom black plates. Final assay volumes in the microwell plate were 300 μL. Generally, gels were prepared within individual wells after mixing the sol (50 μL), buffer (47 μL) and cells (3 μL); M9 minimal media (200 μL) is added overtop after gelation. Similarly, solution samples were prepared from buffer (97 μL) and cells (3 μL); M9 minimal media (200 μL) is added after the corresponding sol-gel derived samples undergo gelation. Blank samples without cells have had an equal volume of cell-free culture added in lieu of bacterial culture. Additives intended to alter the sol-gel derived material are added to the buffer before mixing, whereas antibiotics (i.e., the DNA gyrase inhibitors) intended to induce a cell response were added to the M9 minimal media.

An Infinite M1000 plate reader and the iControl software (TECAN, Männedorf, Switzerland) were used to measure absorbance and fluorescence. Absorbance was collected at 600 nm. Fluorescence parameters were as follows: excitation 488 nm, bandwidth 5 nm; emission 510 nm, bandwidth 10 nm; bottom reads. Gain regulation was applied to real-time fluorescence acquisition, unless otherwise noted, to obtain high fluorescence signal without concern for saturating the photomultiplier tube. Temperature was controlled at 26 ±1°C for all measurements, unless otherwise noted.

Assays were run in triplicate, and the data points were averaged. All assays included blank and promoter-less plasmid (pUA66) controls. The background fluorescence of the *E. coli* cells and buffer was subtracted from the averaged experimental values using the measurements from the cell line containing pUA66; expression levels less than two times above the standard deviation of the promoter-less plasmid are set equal to zero. Induction factors for the drug induction assays are calculated from the background corrected fluorescence of the induced cells divided by the fluorescence of the controls.

2.5 Materials Screen

A materials screen using microwell plates was performed to compare sol-gel composition and *rrnB* expression. Gels were prepared as described earlier with slight modifications to assess the impact of various materials on the promoter expression levels in the collection of cell lines. Samples without additives included PBS or HEPES buffer

mixed with SiNa, and PBS buffer mixed with DGS. Glycerol and GLS were added directly to the PBS before mixing with SiNa. PEG was sensitive to the rapid gelation conditions with PBS, causing flocculation, and instead was added to HEPES buffer before mixing with cells and SiNa. Final concentrations for the additives were 10% glycerol, 2% GLS, or 2% 1kDa PEG.

The base sol-gel composite material studied for the remainder of the project was a mixture of the sodium silicate-derived sol mixed with PBS buffer and cells, without any additives; media was routinely added immediately following gelation. Further references to a SiNa gel indicate this material, while other materials will be designated with a slash and the additive or buffer used.

2.6 Confocal Fluorescence Microscopy

CFM was used for the evaluation of cell growth. Holes of 8 mm diameter were drilled into microscope slides by the McMaster University Glassblowing Shop. Pairs of slides were glued together with epoxy glue, and a cover glass slip was glued with clear nail polish over one end of the microscope slide holes. Gels were made within the slide wells, as detailed above, to a total volume 50 μL, and M9 minimal media was added overtop after gelation. Gels were formed immediately before CFM imaging. CFM images were obtained with a LSM510 microscope and viewed with the Zeiss LSM Image Broweser (Carl Zeiss, Thornwood, NY).

2.7 Viable Cell Counting

CFU determination was used to indirectly observe cell division over time. Solution and SiNa samples containing *E.coli* K12 were prepared in glass vials in the same volumes as those described for microwell assays. Triplicate samples were allowed to incubate at room temperature between 1 and 48 hours in 200 μL of M9 minimal media. After incubation, a series of six 10-fold dilutions into 0.85% w/v NaCl was prepared for both solution and SiNa samples; before dilution, the SiNa gels were crushed with a sterilized metal spatula. Ten microliters of the second through to the sixth dilution was spotted onto a single LB agar plate, supplemented with kanamycin, for each sample. The LB plates were tilted as to spread the aliquots vertically without cross-contamination. Plates are incubated for 16 hours at 37°C. The number of colonies was determined from the lane containing as close to, but less than, 100 colonies.

2.8 Conditions of Bacterial Encapsulation

The constitutive expression of *rrnB* was used to assess the effects of encapsulation within a SiNa and PBS sol-gel composite material using the microwell plate format. PBS was used as the gelation-inducing buffer, and no additives were present. Real-time expression was evaluated over 48 hours for the following samples: solution and SiNa samples as described above; stock LUDOX (40 wt % SiO_2 suspension, pH 9) in place of the sol; diluted LUDOX (12 wt % SiO_2 suspension, diluted with ddH_2O) in place of the sol; solution and SiNa samples containing cell culture diluted by a factor

of ten; and solution and SiNa samples in which the M9 minimal has twice the dextrose added. Additionally, real-time expression of *rrnB* in solution and in a SiNa gel was evaluated over 12 hours at 37°C.

2.9 Electron Microscopy

Cell features were visualized using cryogenic scanning electron microscopy (cryoSEM). Background on cryoSEM of silica biocomposites is described in detail elsewhere.[89] Gels were fixed onto copper specimen holders with Tissue-Tek Embedding Compound (Sakura). Using the Emitech K1250X cryo-preparation unit (Quorum Technologies, East Sussex, UK) samples were plunged in liquid nitrogen slush (-207°C), fractured, sublimated for one hour (-80°C), and gold sputter coated with 20 nm of gold. Samples were imaged with a Hitachi S-570 SEM (Hitachi, Tokyo, Japan), at an accelerating voltage at 10-12 kV, and working distance at 2-5 mm. Images were acquired with Quartz PCI software (Quartz Imaging, Vancouver, BC).

2.10 Crystal Violet Staining

A crystal violet staining procedure was applied to evaluate biofilm content, modified from methods published elsewhere.[90] Solution and SiNa samples were prepared in glass vials as described in section 2.5. Samples were incubated for 24 hours at room temperature before staining; SiNa gels were crushed with a sterilized spatula. Aliquots of dime-sized samples were fixed to precleaned glass microscope slides by running the slide through a flame. Smears are stained for 1 minutes with crystal violet solution, washed

with ddH_2O for two seconds, flooded with Gram's iodine solution, decolorized with 95% ethanol, washed briefly with ddH_2O, and stained with safranin O for 1 minute before one last brief wash with ddH_2O.Cover slips were used to protect the samples.

Slides were viewed with a CH-2 bright field microscope (Olympus, Center Valley, PA), equipped with 10x-magnification oculars and an 100x-magnification oil immersion objective lens, and imaged with type B immersion oil (Cargille). Images were acquired with a PowerShot G11 (Canon, Tokyo, Japan) camera held to the ocular lens of the microscope.

2.11 Promoter Expression and Drug Response

Induction of the promoters described in Table 2.1 was performed in solution and within SiNa gels in microwell plates. NOR or NAL were supplemented into the M9 minimal media so that the final assay concentrations were 125 ng/mL and 8 μg/mL, respectively; control media was supplemented with ddH_2O. End-point measurements were obtained after 16-hr incubation at 26°C. Similarly, the end-point basal expression levels were measured for the promoters described in Table 2.2, and small-molecule induction was not performed.

2.12 Refrigerated Storage

The *rrnB* promoter strain was used to assess mid-term refrigerated storage of cells in solution and in SiNa gels within a microwell plate, supplemented with M9 minimal

media. Samples were stored at 4°C for 1, 3 and 7 days before being performing real-time measurements at 26°C for 24 hours.

2.13 Microarray Fabrication

A BioRAPTR FRM Microfluidic Workstation (Beckman-Coulter, Brea, CA) was used to deposit 100 nL volumes onto a Greiner Bio-One 96-well, glass bottom Sensoplate. Wells contained a maximum of three array elements, each containing 100 nL of SiNa sol and 100 nL of PBS buffer with cells expressing *rrnB* promoter-linked GFP, for a total of 200 nL. Minimal media was added between 10 and 30 minutes after printing. The plate was imaged with a NovaRay Microplate and Slide Imaging System (Alpha Innotech, San Leandro, CA). The excitation and emission were acquired at 478 and 538 nm, respectively. Exposure settings were automatic and focus settings were set manually until real-time images appeared sharp. Images were acquired at a 4 micron resolution.

Chapter 3 | Results and Discussion

3.1 Effect of Sol-Gel Composition on Cell Viability

Initial studies assessed several silica-hybrid materials for entrapment of cells carrying the *rrnB* promoter-linked GFP reporter genes to assess which materials retained cells in a viable state. Sodium silicate-dervied sol-gel materials can provide a biologically inert and optically clear matrix for entrapment. The ion-exchange method for preparing the sol from sodium silicate allows for good control of the ionic strength, as opposed to alkoxide-derived sols which are mixed with concentrated acid before use. Furthermore aqueous and sugar-modified sols (e.g., DGS) do not contribute any alcohol content to the gel.

Glycerol is a protein stabilizer used for microarray screening of proteins,[79] and is beneficial in short term storage of cells;[75] supplemented glycerol and the DGS sol, which releases glycerol upon gelation, were considered for these reasons. GLS and APTES were selected since they are capable of passivating the matrix, neutralizing the matrix and improving the ability of small molecules to pass through without adhering to the anionic silica matrix. PEG was used to increase pore size, although increasing pore size reduces the optical clarity of the gel larger pores may be necessary to accommodate the bacterial cells. PBS was used for most of the compositions since it is a cell-friendly buffer and the phosphates allows for rapid gelation times once mixed with sols. HEPES was used for a slower gelation time; despite having the same final concentration, HEPES will not induce

gelation as fast as phosphate buffers. HEPES buffer was also used in the APTES and PEG compositions to avoid flocculation of samples, i.e., particulate silica colloids which precipitate out solution without any formation of a coherent gel.

The expression profiles for the various materials, including the non-gel solution sample, are summarized in Figure 3.1. This work was done in monoliths within a microwell plate with a volume of 100 uL; 200 uL of minimal media was added after gelation to provide a nutrient source. *E. coli* cells were grown to the early exponential phase before fabricating monoliths. The results illustrate that several compositions, particularly SiNa and DGS, have generated similar fluorescence signals from GFP as the *E. coli* suspended freely in solution. This is counter-intuitive since it has long been suggested that cells are incapable of dividing within sol-gel materials, and as such would produce less total GFP within the gel. However this is also the first instance in which a direct comparison between bacterial cells entrapped in a silica matrix and in solution has been made. It is also possible that a massive over-expression of the *rrnB* promoter occurs upon entrapment, and requires further investigation.

The SiNa matrix prepared with PBS appears to be the most conducive towards supporting *E. coli* cells, as the fluorescence produced closely mimics the solution assay and was greater at all time points. The DGS matrix similarly maintains a high level of

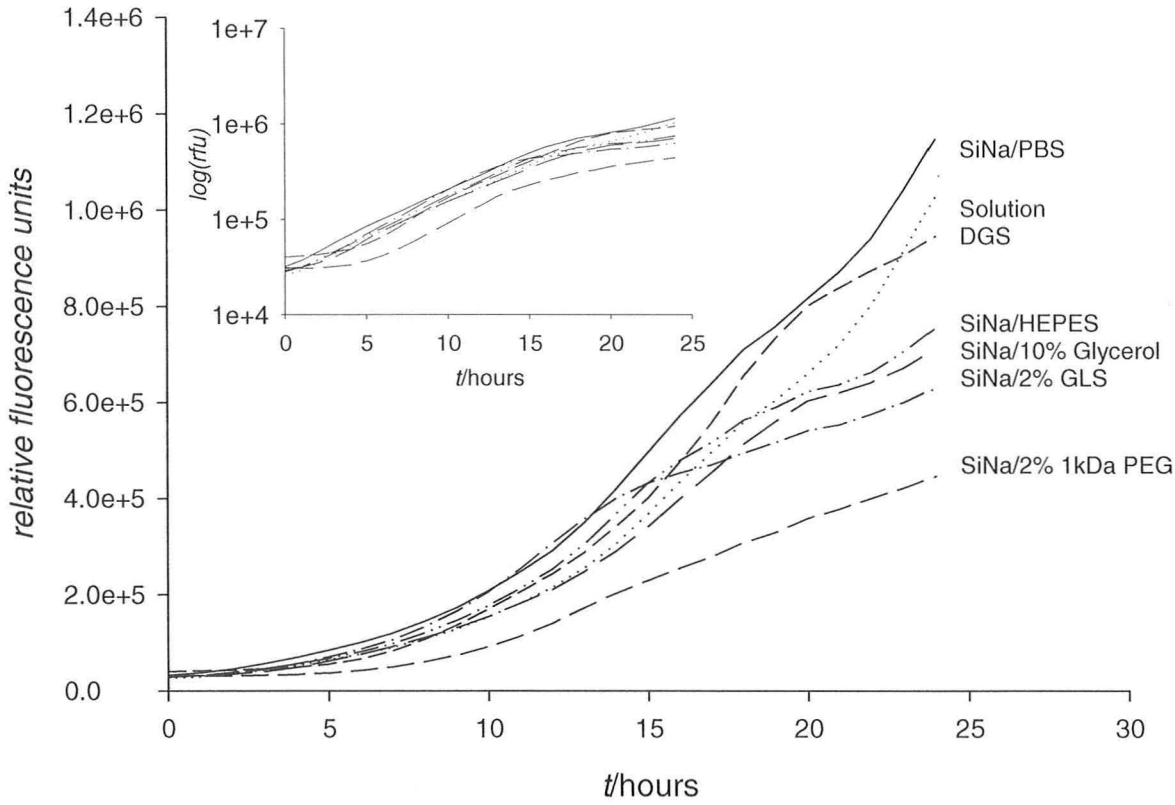

Figure 3.1 Real-time expression profiles of the *rrnB* promoter in solution and entrapped in various silica and silica-hybrid matrices. Presented in logarithmic scale within insert.

fluorescence, but tapers towards the end of the 24-hour period. Most surprisingly, the SiNa matrix prepared with HEPES had a much lower expression level than its PBS counterpart; the HEPES buffer has a longer gelation time when mixed with SiNa, approximately 40 min, whereas the phosphate buffer induces much faster gelation times. The longer gelation time may have unfavourable effects on the *E. coli* cells.

Possible leaching of cells from the silica-solution interface was also assessed for interference with assay measurements. At the end of incubation periods or real-time expression measurements, wells containing sol-gel samples with media were measured for fluorescence of the constitutively fluorescent *rrnB* promoter strain; the media overtop the gel was moved into an empty well and both the media and the gel were remeasured. The entire fluorescence signal was recoverable from the media-free sol-gel sample, within one standard deviation (data not shown). Leaching tests were consistently performed for a sample of the microwell plate assays, including alternative materials used, and the leaching fluorescence was consistently insignificant.

The unmodified SiNa matrix prepared with PBS was investigated further since it was shown to have the most similar expression profile for the *rrnB* promoter in solution, and produces the simplest silica network while releasing only water upon gelation. Thus experimental conditions report solely on the effects of entrapment within a silica matrix and not on the effects of functionalized silanes, polymers or additives. Since the SiNa

sol-gel composition will be used for screening, and cell division is a valuable in screening, the division of entrapped cells should be investigated.

3.2 Cell Division within a Silica Matrix

As mentioned previously, cell division has yet to be shown within a silica matrix,[91] however the progression of the GFP production over 24 hours appears similar to cells growing freely in solution (Figure 3.1). Time-lapse CFM was previously used to image cells within a thin film, concluding that no division was visible.[74] CFM was similarly applied here but to image cells within a SiNa monolith instead of a film; imaged cells were those in close proximity to the bottom of the gel (Figure 3.2). The gel was immersed with media and should have a similar GFP expression profile as in Figure 3.1.

Fluorescence images show cells between two and ten hours in the same area and plane. The cells were not mobile, and do not demonstrate a large change in the volume occupied. However, it is difficult to determine the number of cells in a single pore, that is, there can be multiple cells within one pore that is not discernable with CFM. The continuous time-lapse fluorescence photography of the cells proved difficult because the gel undergoes continuous crosslinking over long periods of time, causing the gel to shrink and the cells to move with respect to the microscope's plane of view. Furthermore, time-lapse CFM, especially with multiple images being obtained in the Z plane, resulted in

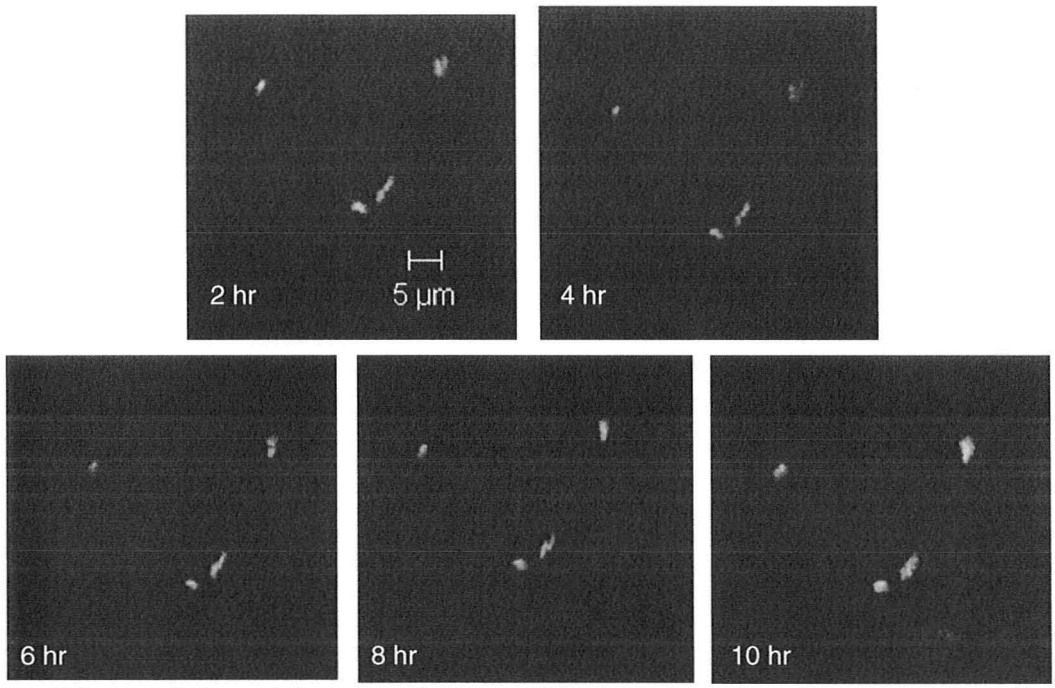

Figure 3.2 From left to right, top to bottom: CFM images of GFP-expressing *E. coli* cells after 2, 4, 6, 8 and 10 hours

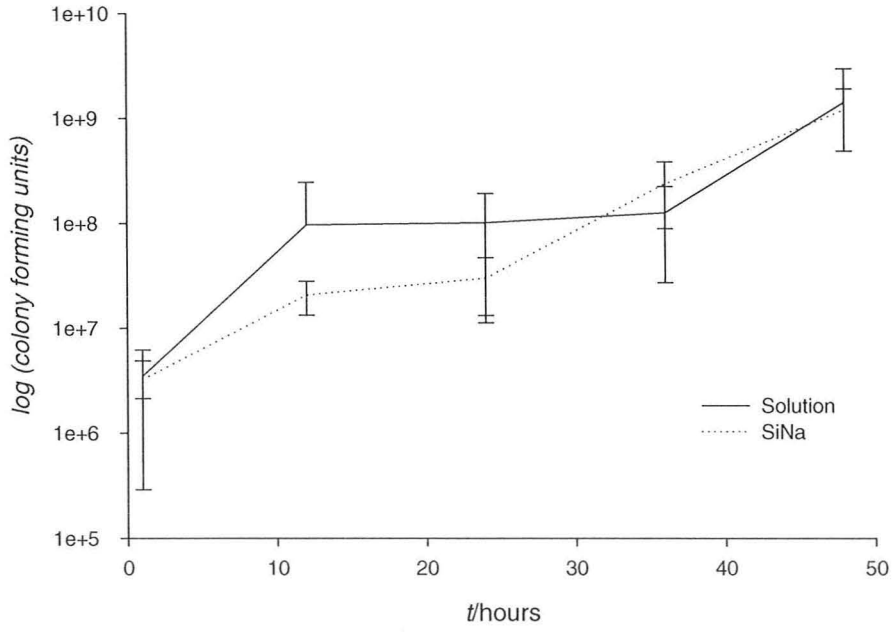

Figure 3.3 The number of cfu from solution and silica samples over 48 hours

photobleaching of the GFP. The CFM did not provide a direct indication that growth occurs or does not occur within the silica matrix.

Plate counting methods were applied to indirectly determine the number of viable cells present in both solution and SiNa gels. Cells were incubated in either solution or in silica mimicking the microwell plate assay conditions described earlier. Samples were tested in triplicate at 12 hour intervals over 48 hours, at room temperature, and unique samples were used for each time interval. The soft silica monoliths were readilydisrupted with a spatula; the gels do not become dry or brittle since they remain immersed in media. Some bacterial cells may remain enclosed in silica after disruption and thus the viability of encapsulated cells may be under represented.

Using plate counting method of cells entrapped in gel and those in solution, it was clearly observed that there are a comparable and increasing number of cells within each sample (Figure 3.3). A 100-fold increase in the number of cells was observed within each of a SiNa monolith and the solution control after 48 hours; these samples were prepared in the same volumes as the microwell plate assays and thus the number of cells should be representative. This data conclusively shows that cells are capable of division within the silica matrix otherwise the number of cells would not increase so dramatically, or at all. Cells are randomly dispersed when they are suspended into a gel however, based on the CFM data, daughter cells are isolated to the pore in which the mother cell is situated. The observed cell growth supports the high *rrnB* promoter expression data; the

expression levels in the SiNa monolith and in solution were comparable since the cells divide at a similar rate in both conditions. However, a 48-hour period of incubation before CFM imaging may be useful in visualizing the effects of growth after extended incubation. The plate counting method indicates that the cell concentration increase roughly 100 fold, but it has yet to be seen if such a number of cells will occupy space within the silica gel in the same way they do after ten.

It is possible to further describe the changes that affect entrapped bacteria in a silica matrix by altering assay conditions, as opposed to altering the matrix composition, while measuring real-time GFP expression.

3.3 Conditions of Bacterial Encapsulation

In the microwell plate assays described here, the assay contains cells that are grown to an optical density at 600 nm of approximately 0.2, representing the early exponential phase. Parallel assays contained cells that were diluted to 1/100 and 1/1000 of the final assay volume (Figure 3.4). At the end of a 48-hour incubate period, the fluorescence levels of the parallel experiments reach similar values the respective solution or SiNa samples. This suggests that the cells can grow freely until the nutrient source is exhausted within the matrix, similar to the solution assays, resulting in a comparable number of cells after a long enough period of time.

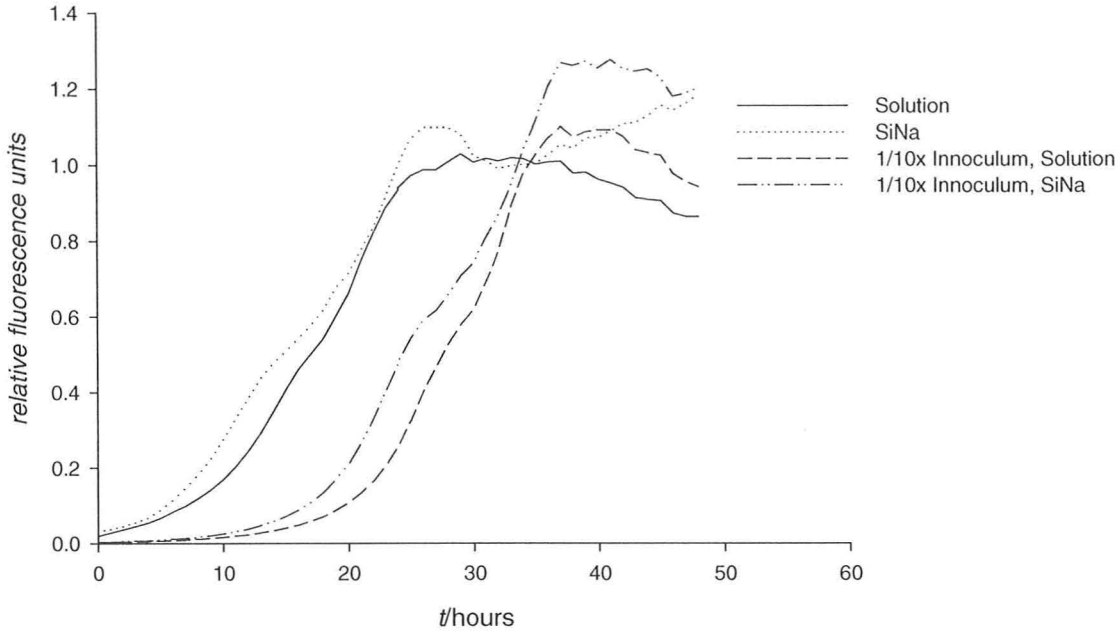

Figure 3.4 *rrnB* promoter activity for cells at normal and 10-fold diluted cell concentration

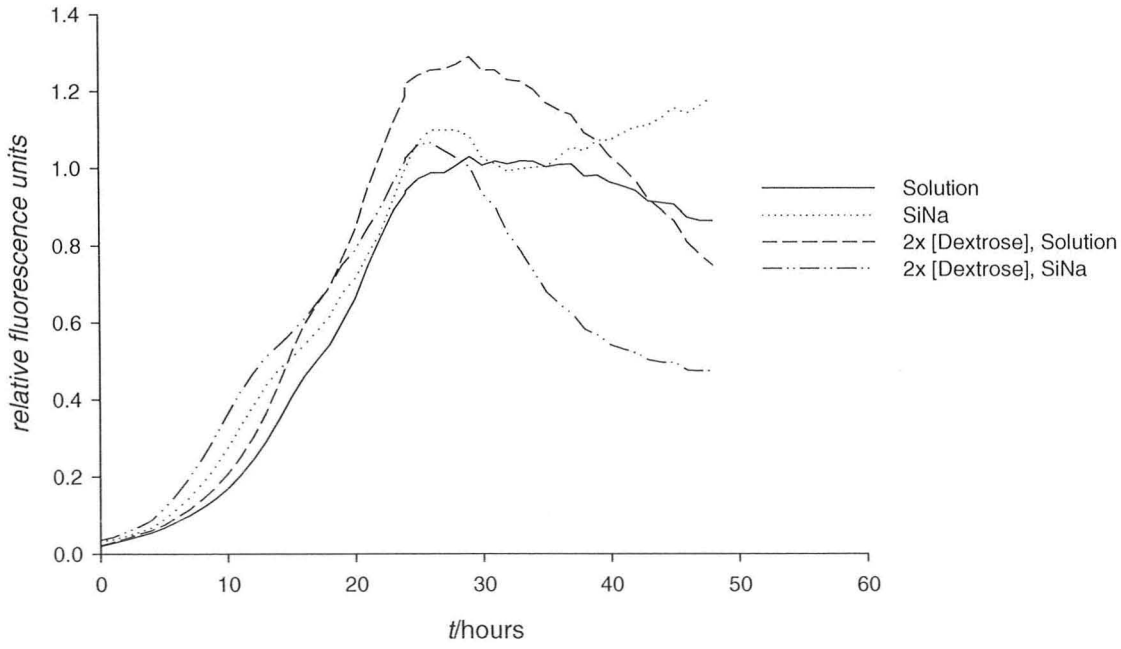

Figure 3.5 *rrnB* promoter activity at normal and 2-fold dextrose concentrations

The effects of a higher concentration of the initial carbon source was assessed by monitoring parallel assays which contained the same starting inoculum, but with the addition of samples doped with twice the concentration of dextrose (Figure 3.5). While the fluorescence expression for solution for the high-dextrose sample shows higher GFP expression than the low-dextrose sample, the SiNa samples show the similar maximum fluorescence in both high and low carbon source conditions. The death phase is pronounced in the tail of the fluorescence signal for both solution and silica samples with high dextrose. It's possible that there is a maximum capacity within the silica monoliths to contain active cells; the bacteria can grow freely within a pore until further division cannot occur, whereas the solution assay is unlimited in space for division.

A third 48-hour experiment was run in parallel with the aforementioned assays, but here examined the effects of colloidal silica. Colloidal silica was used to observe the effects of non-gel forming silica onto the *E. coli* cells. Both 40 wt % colloidal silica (LUDOX, pH 9) and 12 wt % LUDOX (at the same final silica content as the SiNa gels, pH 9) were used here (Figure 3.6). Immediately apparent is that the high LUDOX sample does not allow for cell growth, whereas the low LUDOX sample ultimately has a higher fluorescence signal than either the solution or sol-gel samples. It should be noted that LUDOX is prepared with an isothiazolin biocide, and likely contributes to the loss of signal. The low amount of colloidal silica does not appear detrimental to bacterial cells, and removes the physical restriction imposed by the solid SiNa gels.

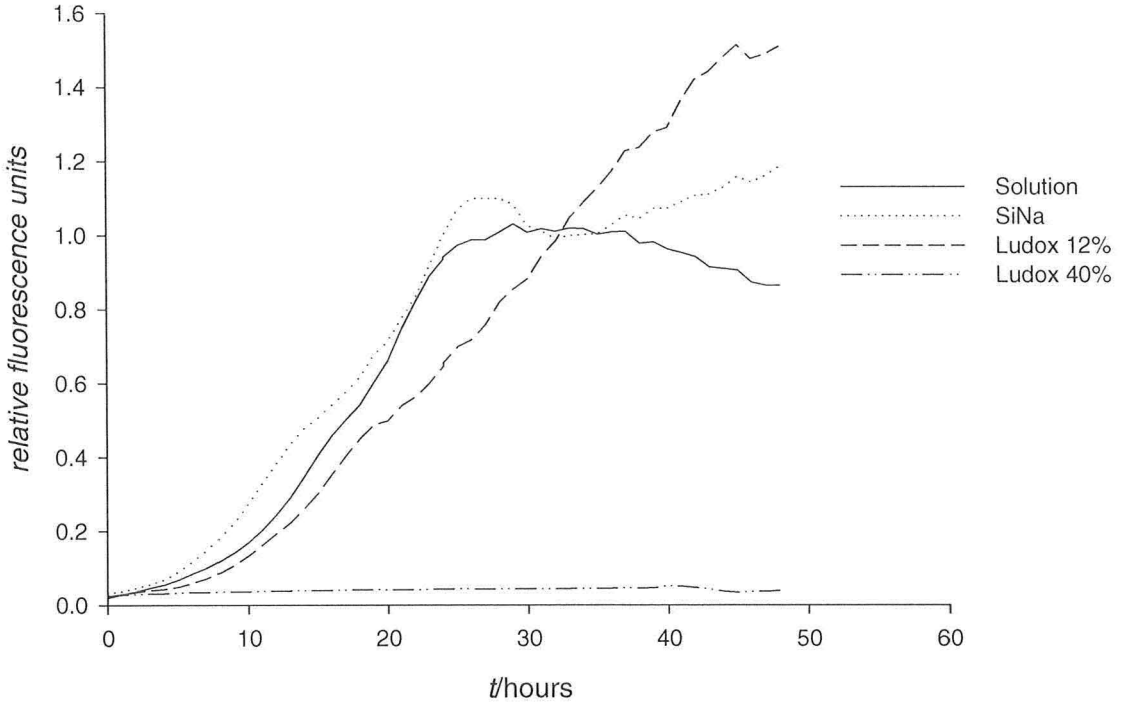

Figure 3.6 *rrnB* promoter activity for cells in solution, SiNa and LUDOX samples

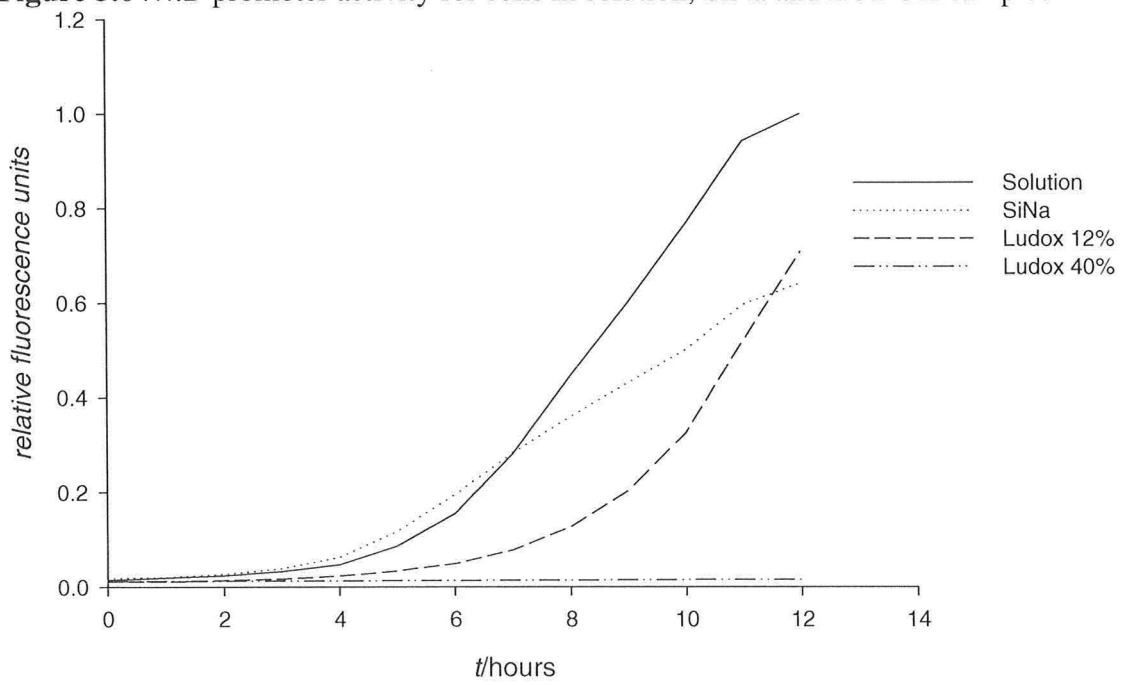

Figure 3.7 *rrnB* promoter activity for cells in solution, SiNa and LUDOX samples at 37°C

The microwell plate assay was repeated for solution, SiNa and LUDOX samples, with the temperature controlled at 37°C during the course of the fluorescence observation (Figure 3.7). This experiment was limited to 12 hours to avoid measurements once media has evaporated. After a period of 7 hours, the signal from the solution becomes larger and has a greater slope than SiNa. Previously it was observed that the population of cells would reach a maximum capacity within the gel and then taper off in signal while remaining comparable to solution, instead a noticeably slower generation of the fluorescence signal is observed in respect to the solution assay, despite more favourable conditions for *E. coli* growth. These results reflect the rate of diffusion within a silica matrix; it is possible that the cells metabolize the locally available carbon source, and the growth rate becomes contingent on the rate of diffusion. The fluorescence signal observed for the low LUDOX sample shadows the solution sample, neither of which bear concerns for diffusion rate. The presence of a biocide in LUDOX may mask the effects of the colloidal silica; it would be ideal to synthesize colloids without the presence of any antibiotic to better visualize its effects.

The data thus far does not reflect the physical characteristics of the entrapped cells. Electron microscopy methods has been previously applied to visualize entrapped bacteria.[89] CryoSEM can similarly be used here to observe the physical features of encapsulated cells.

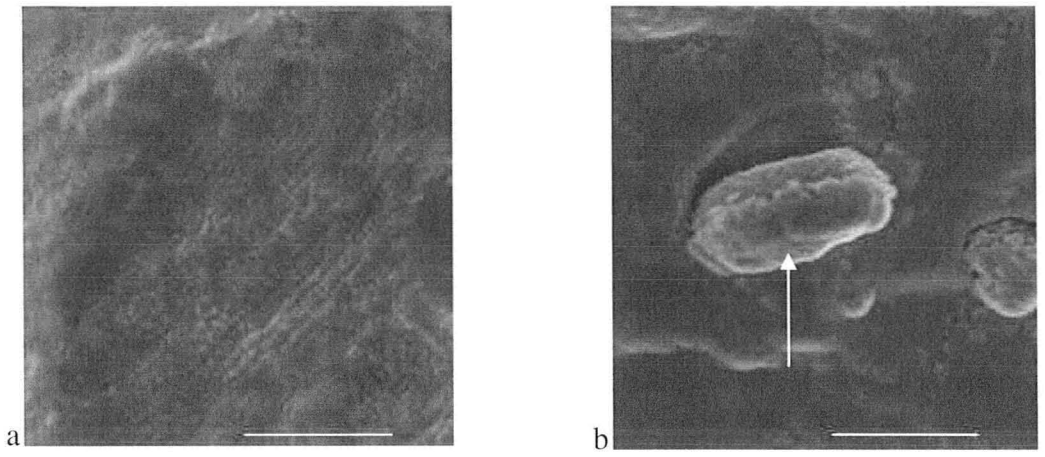

Figure 3.8 CryoSEM images of silica hydrogels incubated overnight: a) SiNa without cells; b) SiNa with cells, arrow points to sign of entrapped cells dividing arrows point to pores containing groups of cells. Scale bars are 6.0 μm

3.4 Microscopy for Cell-Surface Features

CryoSEM was used to preserve the water structure of the gels; alternative SEM preparation methods, e.g., heating or alcohol exchange, cause significant shrinkage of the silica matrix from the loss of water and may not reflect a similar environment as the assay conditions. SiNa samples were prepared with and without cells and incubated at room temperature (21°C) overnight, and analysed with cryoSEM the following day (Figures 3.8b and 3.8a, respectively). The SiNa gel formed a particulate matrix with mesopores. The cell-doped SiNa gel showed a pocket containing multiple cells in the middle, and a cell to the right; a division line appears in the middle of what appears to be two cells at the forefront of the image, however there is a coating of the hydrogel around these cells.

From the cryoSEM data, it is most important that distinct cells embedded within gel matrix are visible; and the separation of two cells in the same pore is visible. The

silica hydrogel may have template the encapsulated cells, or the *E. coli* cells are creating a biofilm layer in response to entrapment. The texture of the film appears similar to the texture of the surrounding silica matrix, however it is possible that the cells produced a carbohydrate biofilm upon entrapment.

A crystal violet (Gram) staining method was applied to detect the presence of carbohydrate biofilm. While a wheat germ agglutinin-fluorophore conjugate may normally be more efficient in detecting exopolysaccharides,[92] a crystal violet and safranin stains were selected since they are much smaller in size and can more readily diffuse through a silica matrix than the agglutinin antibody.

Single cells were visible from incubated solution and silica samples (Figure 3.9a and 3.9b, respectively). Cells incubated in solution appear pink from safranin staining, representing a lack of biofilm. The cells incubated within a silica matrix also image as pink bodies, but appear relatively darker. Cells which positively stain with crystal violet do so because an acetone or alcohol wash does not penetrate the carbohydrate outer layer, and the following safranin stain does not visualize. Here the safranin stain does visualize within the cell following the crystal violet staining and wash. Also, the silica sample visibly retains the purple stain in cell free areas, suggesting that the silica will non-

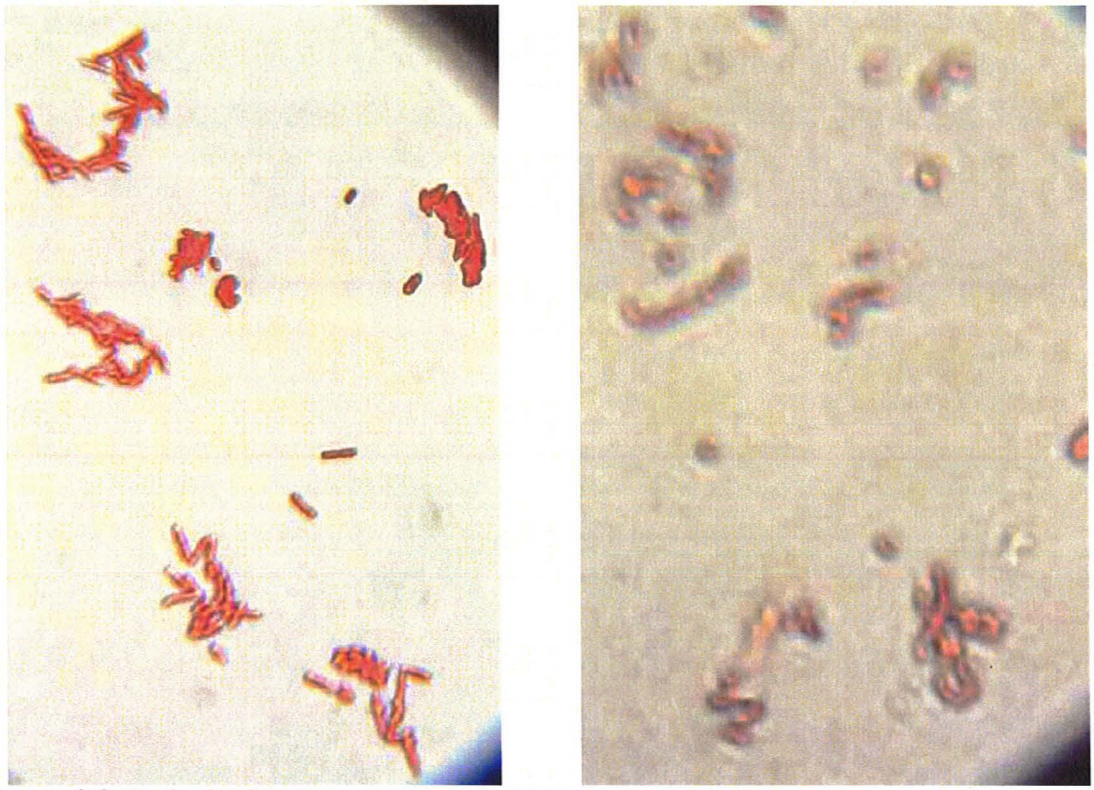

Figure 3.9 Optical microscopy
mages of *E. coli* cells after 24 hours incubation in solution (left) and silica (right)

specifically attract the dye but will still freely allow the alcohol to diffuse through the matrix and remove any crystal violet stain from the cells. The presence of the pink safranin dye within the encapsulated bacteria indicates that there is no biofilm being formed.

3.5 Promoter Response to Sol-Gel Encapsulation

A set of GFP-linked promoters were also examined for physiological differences in solution and in silica, as selected for, and summarized by, their descriptions in Table 2.2. An increase in promoter expression was detected from the promoters *pyrB*, *rpoE*, *otsB*, *rpoH*, *cspD*, and *ompX* (Figure 3.10), however, from the previous real-time

fluorescence measurements, it was observed that the fluorescence signal generated from SiNa was as great as 2.4-fold the GFP signal generated from solution for the same promoter at the same time. Similarly, promoters which have greater basal promoter activities in solution have a proportionately greater signal in SiNa. If the promoters were to be induced as a result of sol-gel encapsulation, the difference in fluorescence signal should be at least two-to-three fold greater than the control to reflect any significant changes in promoter activity.

The observations here support that the sol-gel encapsulation of the bacterial cells has not affected promoter activity and has not induced any abnormal response. As organisms are capable of surviving through various challenges, it is not necessarily understandood as to how *E. coli* adapts to the change in environment. It is possible that the silica network may interact directly with the extracellular matrix, impede or halt cell division, or induce heat shock, oxidative, osmolyte or other stress response. Although it may seem unlikely that some stress responses can be induced upon entrapment, the mechanism of stress response can often be general in nature; for instance a heat shock response can be induced by ethanol, where the ethanol increases the presence of abnormal unfolded proteins in the cytoplasm and mimics a scenario where the cell would be in a hot environment.[93] However, while some of the stress-related promoters appear induced, none of the promoters selected demonstrate induction levels great enough to

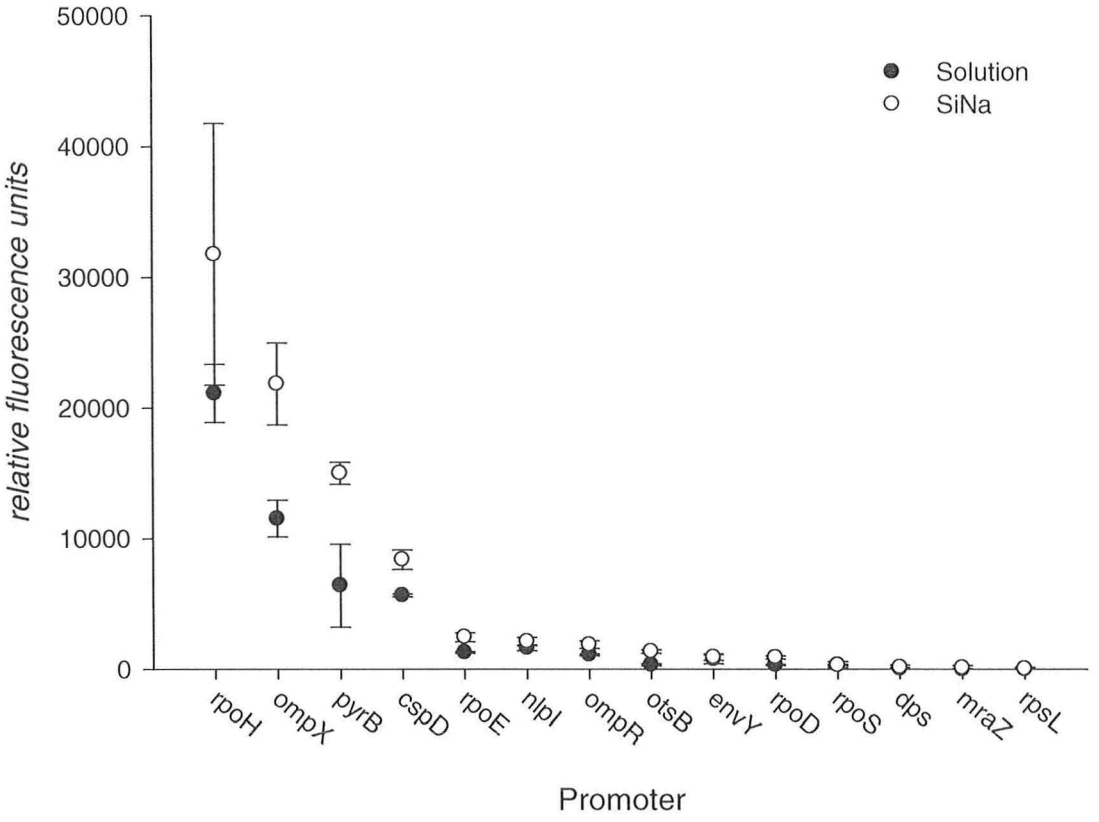

Figure 3.10 Fluorescence from various GFP-linked promoters after 16 hours incubation in solution and silica

communicate a specific response. Thus, it remains to be shown that there is any inadvertent affect from the silica matrix on promoter activity. A comprehensive solution may be to perform a global analysis screen on the cells in solution and in silica. While the selection of promoters analyzed here represent a small survey of available promoters, a global screen of the entire 1900-GFP-linked-promoter library may, and any positive hits, i.e., that responds to silica entrapment, can be analyzed in order to further describe the effects of silica entrapment on *E. coli*.

3.6 Long-Term Storage

In order to draw contrast to solution, and since it pertains to the fabrication of microarrays, the refrigerated storage of sol-gel entrapped cells was examined. SiNa and solution samples were prepared in microwell plates with minimal media and stored at 4°C for 1, 3 and 7 days. Afterwards real-time expression was immediately measured at 26°C (Figure 3.11). As the storage time increases, the difference between the solution and SiNa samples becomes drastically larger, and after a week the solution sample manages to generate less than half the fluorescence signal generated by sol-gel entrapped bacteria. This was expected since over year-long storage was previously observed with a similar SiNa gel, but without any comparsion to solution.[75]

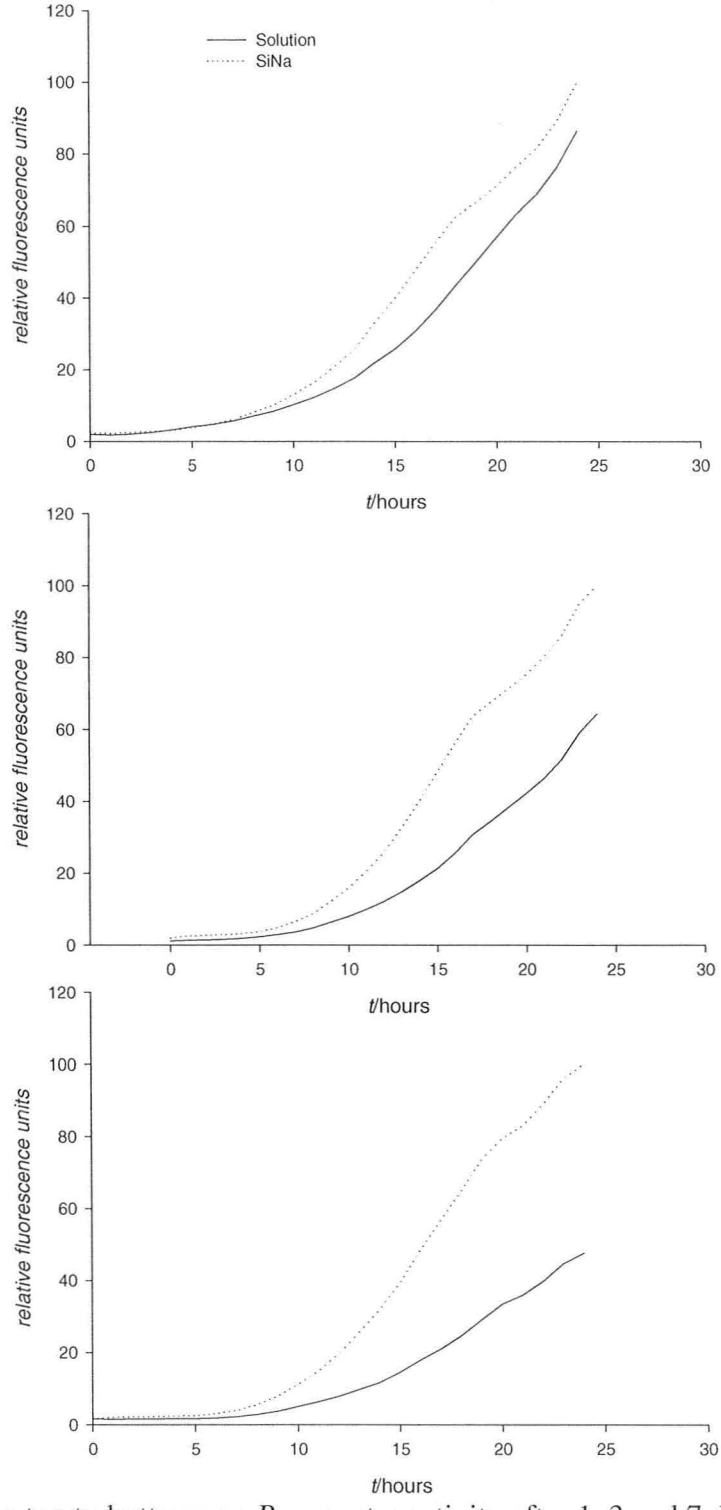

Figure 3.11 From top to bottom: *rrnB* promoter activity after 1, 3 and 7 days of storage

3.7 Comparative Screening of DNA Gyrase Inhibition

The purpose of describing the encapsulation of bacteria is to ultimately apply this towards compound screening. It is important to assess how screening cells within a silica matrix may alter from common screening practices. The cell response to small molecules is assessed here in microwell plates. A selection of promoters were chosen to be induced with NOR and NAL, both quinolone derivatives and DNA gyrase subunit B inhibitors, from previous unpublished work completed by Falconer and Brown suggesting that they may be up- and down-regulated by these antibiotics (Shannon Falconer, Dr. E. D. Brown Lab, Department of Biochemistry and Biomedical Sciences, McMaster University). The promoters are described in Table 2.1. The induction factor describes the ratio of fluorescence signals from the induced cells over the non-induced controls.

Upon induction with NAL, half of the tested twelve strains showed a greater response in GFP expression levels (Table 3.1). Promoters *recA*, *recN, suiA, lexA, rmuC* and *yfbM* all showed the greatest increase in fluorescence signal with the addition of NAL, both in sol-gel derived materials and in solution. Similarily, *recA, recN*, and *suiA* were induced by NOR in silica and solution, and *lexA* showed a significant increase in the sol-gel matrix only. All reporter strains which showed a change with the addition of NOR or NAL had a higher fluorescence response in sol-gel derived materials than in solution, the only exception being *valV* which shows a 3-fold increase in promoter activity after induction of NOR in solution, but not in silica. Signal induction was not hampered as a result of encapsulation, and expression levels were often higher for induced cells. As

mentioned earlier, it has been previously shown that cells are better preserved and protected within silica materials, which might suggest why the trends for higher GFP-fluorescence was observed in silica matrices.

The real-time observation of the *recN* promoter was observed for various concentrations of NAL in both solution and SiNa (Figure 3.12). Results between solution and SiNa were consistent with previous observations; the same trends were followed for every concentration, and silica samples were consistently higher. The high signal generated by the promoter in silica allows for greater signal-to-noise ratios at all concentrations.

Table 3.1 Promoter induction factors for the response to DNA gyrase inhibitors. Performed in triplicate.

	NAL Induction		**NOR Induction**	
Promoter	**Solution**	**SiNa**	**Solution**	**SiNa**
recN	63 ± 14	90.5 ± 3.2	9.8 ± 0.4	11.9 ± 0.6
sulA	24.9 ± 0.7	35.5 ± 1.0	9.1 ± 2.5	18.9 ± 4.4
recA	17.9 ± 1.4	24.9 ± 0.7	15.4 ± 1.6	19.5 ± 4.6
lexA	10.8 ± 4.0	15.2 ± 8.1	1.8 ± 0.2	5.6 ± 0.5
rmuC	6.9 ± 0.5	11.4 ± 0.6	0.90 ± 0.05	2.6 ± 0.4
yfbM	3.8 ± 0.5	3.87 ± 0.03	0.10 ± 0.01	0.77 ± 0.06
yjbJ	1.7 ± 0.2	1.8 ± 0.1	0.34 ± 0.03	2.3 ± 0.6
valV	1.6 ± 1.7	2.6 ± 1.7	3.2 ± 0.4	1.4 ± 0.3
ybhE	1.5 ± 0.3	2.0 ± 0.1	0.16 ± 0.01	0.39 ± 0.04
minC	1.4 ± 0.1	1.64 ± 0.03	0.11 ± 0.01	0.5 ± 0.1
osmE	1.3 ± 0.1	1.49 ± 0.05	0.25 ± 0.04	0.67 ± 0.09
nmpC	1.2 ± 0.8	1.5 ± 0.9	0.15 ± 0.01	0.47 ± 0.06

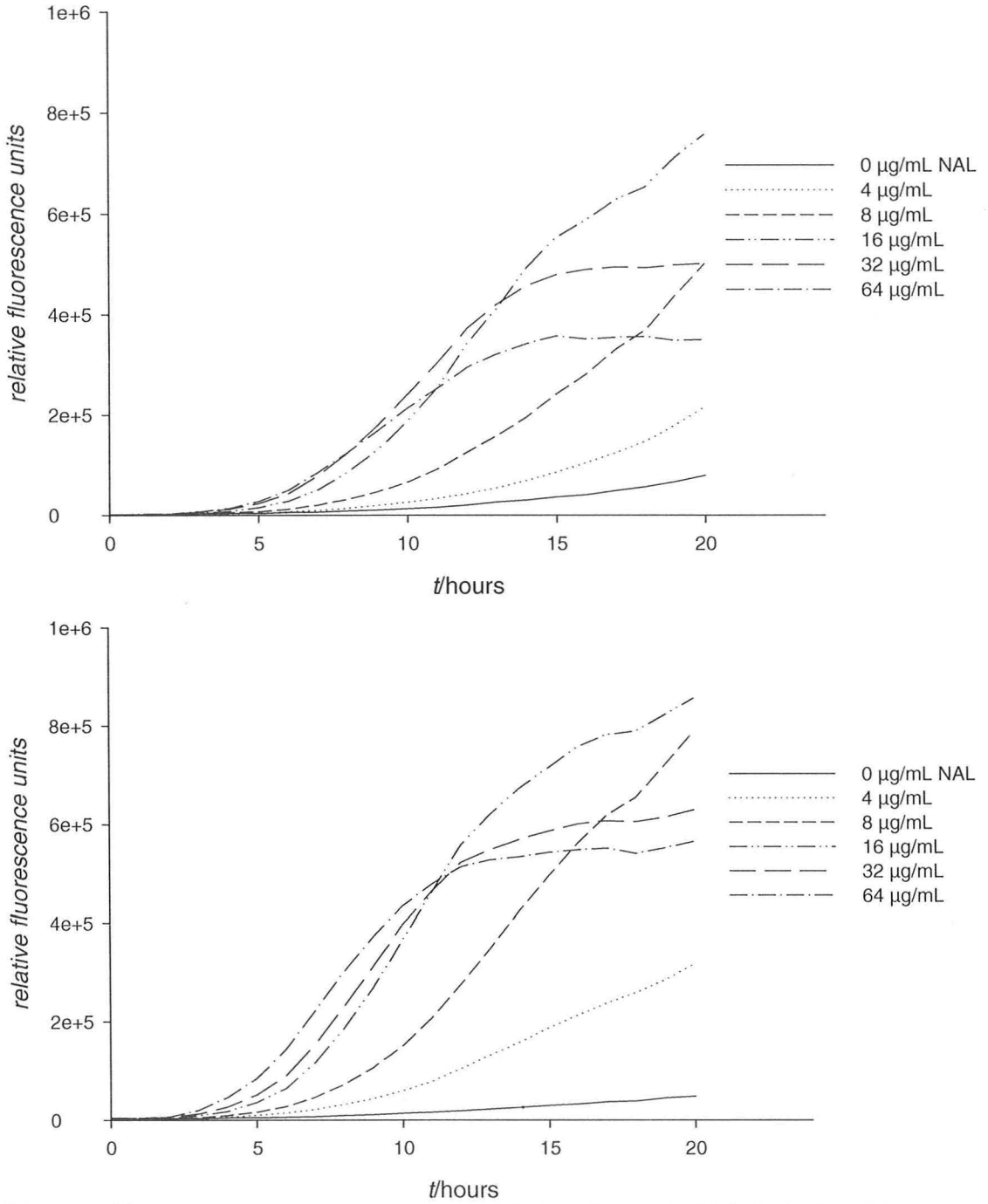

Figure 3.12 Dose dependent response to nalidixic acid on the GFP-linked *recN* promoter in solution (top) and silica (bottom)

3.8 Non-Contact Array Fabrication

There are two competing processes that must be taken into consideration when printing sol-gel derived microarrays: silica crosslinking and dehydration. As these two processes continue, the resulting material becomes increasingly brittle and becomes susceptible to cracking. Conversely, the early addition of media to a buffer- sol mixture will dilute the gel resulting in the loss of spatial control and partially formed array elements. Modern microarray printers can dispense sub-nanolitre volumes, exaggerating the effects of gelation observed in bulk materials.

Contact pin printers dispense pre-mixed solutions, and as such require long gelation times (e.g., with buffers such as HEPES, in low concentrations) to avoid gelation within the instrument; this results in a slow improvement of structural integrity over time since polycondensation of the matrix is slow. A collection of pin-printer-compatible sol-gel compositions was described by Monton *et al.* for protein microarrays; substrates were added by means of over-spotting solution with a larger pin onto individual array elements.[79] The method of over-spotting reduced the effects of cracking by adding a volume of solution greater than the volume of the gel. Unlike cells, the protein microarrays do not require media to remain active, and as such array elements remain spatially secure during the assay.

Due to the high gelation time of the SiNa and PBS derived sol-gel composition described here, non-contact drop-on-demand printers are better suited to printing these

materials, in which the sol and buffer are not premixed but instead form a gel when mixed on a surface. Ink jet printers are the non-contact technology used to print sub-nanolitre volumes. Ink jet printers for material deposition use either thermal or piezoelectric drop-on-demand printing methods; the former can only print volatile mixtures through an interface which heats up to deposit materials, whereas the latter charges a piezoelectric material for ink deposition. Of the two types of instruments, the piezoelectric microarray printer is, in theory, advantageous since there is no restriction on the use of materials.

In lieu of a piezoelectric printer, a microfluidic liquid handler (BioRAPTR workstation) capable of reliably dispensing 100 nL volumes into microwell plates was used. The microfluidic workstation uses pneumatic pressure to dispense solutions without contact into high-density microwell plates (although replaced here by 96-well plates for microarray fabrication), and is a model for piezoelectric dispensing. Demonstrated here is an array element printed from a sodium-silicate-derived sol and PBS buffer containing *rrnB* promoter-linked-GFP *E. coli* cells (Figure 3.13). In trial runs with the microfluidic workstation, the array element components were printed at 100 nL each, for array elements at a final volume of 200 nL. A maximum of three array elements were printed into a single well of a 96-well plate; glass bottom plates were used to improve adhesion

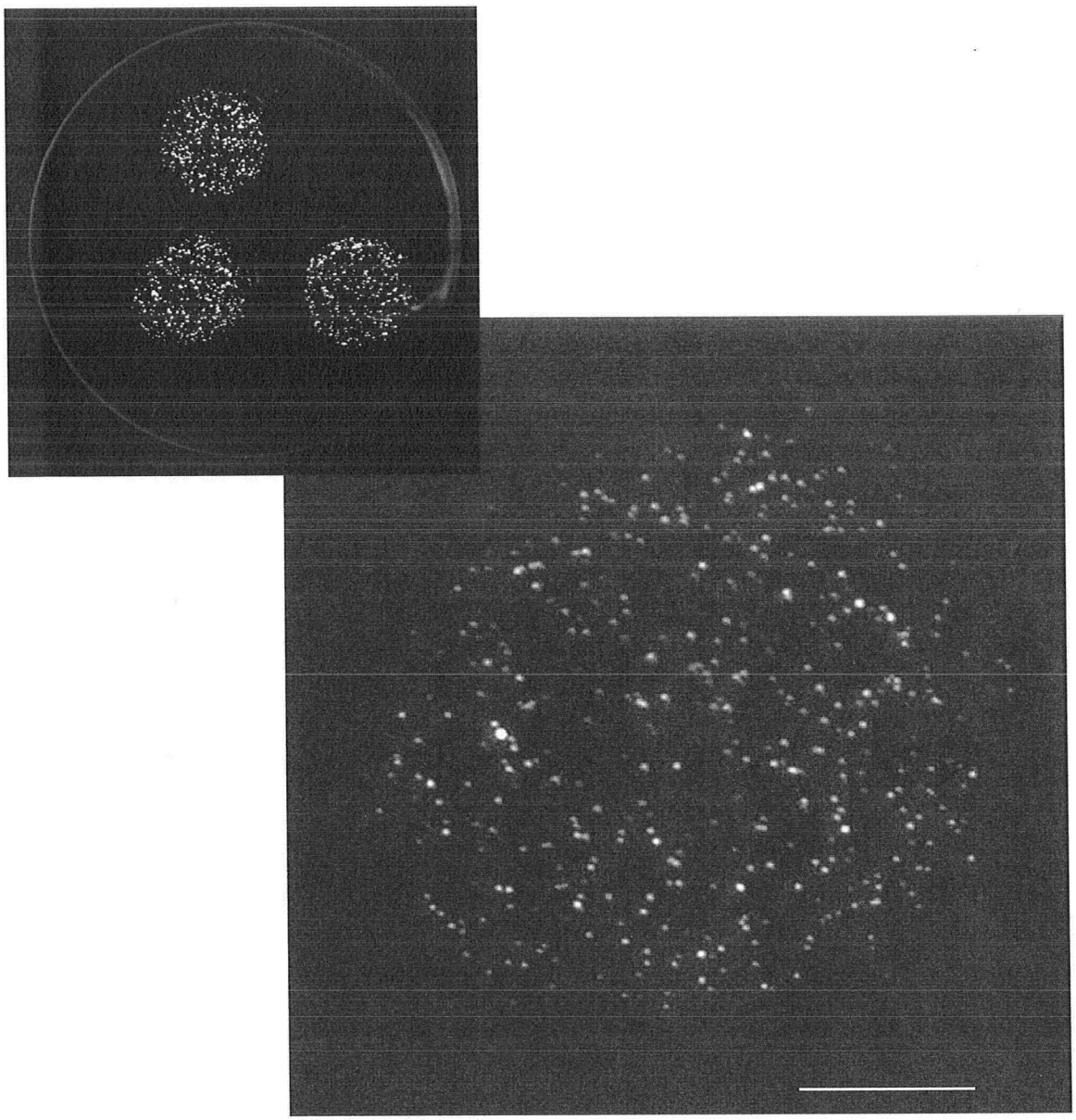

Figure 3.13 Single-well Array of *rrnB* promoter-linked GFP expressing cells entrapped in silica matrix (top left). Single array element enlarged (bottom right). Scale bar represents 0.5 mm.

with the silica matrix. It took less than a minute to print 288 array elements from two nozzles.

Parts of the array were allowed to gel for 5 through to 30 minutes before the addition of media. The array elements were imaged after 16 hours at 30°C. Not all array elements remained coherent: in some wells, two array elements bled into each other after gelation, and array elements that were not allowed to undergo gelation for at least 10 minutes did not form. Array elements that did not have any media added to them cracked after three hours. The fluorescence signal is confined to the area in which the material was printed, and thus leaching is not observed from the array elements. The large dispensed volumes, and the low density of array elements per well are not indicative of a microarray; the instrumentation used to realize the printed array is not intended for microarray printing. Additional attempts are printing similar arrays have not been successful. However, the array elements produced and the opportunity to print materials with fast gelation times are conducive in developing a methodology for non-contact piezoelectric drop-on-demand printers. The fast gelation times allow the user to add media to the array sooner, before dehydration of array elements occurs.

From the research described in this thesis, optimization of piezoelectric microarray printing for array elements of *E. coli* cells entrapped in SiNa gels can be quickly discerned by performing a two-dimensional assessment of printable volumes and time allowed for gelation. Printing a variety of volumes and volume ratios of the array

components in one direction, and varying the time allowed for array elements to gel before the addition of media, as was performed here with the BioRAPTR microfluidic workstation, but with a single setting the volume dispensed. Performing such a screen will allow future users to reap the benefits of using fast-gelling, cell compatible material such as the sodium-silicate sol and PBS composition entailed here.

The sodium silicate-derived material has reproducibly shown successful entrapment of viable cells in microwell plates, and fluorescence promoter signals have been consistent in multiple trials. The microarray format for this material was successfully demonstrated for the end-point fluorescence expression of the *rrnB* promoter, however subsequent attempts at optimizing and printing arrays with the BioRAPTR workstation have failed as a result of printing inaccuracy, i.e. the BioRAPTR is not adept in low-volume dispensing for microarray fabrication and is instead suited for high-density microwell plates.

Chapter 4 | Conclusion

The entrapment of E. coli cells in SiNa matrices provides a suitable environment in which the cells can adapt and remain viable, and respond to the presence of small molecules in an appropriate manner compared to side-by-side solution assays. The results here show that cells behave in a similar fashion as they do in solution; the silica matrix is supportive for cell viability. Cells can grow within the pores of the silica matrix. The silica matrix does not appear to induce any undesired effect on any of the promoters screened. The work here could be applied to a larger screen, such as a global analysis of the *E. coli* promoter collection in solution and silica to elucidate any greatly significant physiological changes that were not detected here.

The sodium silicate-derived composition has several desirable features as a compatible material, shown here to maintain high levels of fluorescence consistent with induction in solution. The minimalistic material is preferred here as there are fewer possibilities for interference with cells, and fewer limitations with respect to preventing flocculation during the addition of certain additives or controlling gelation time. Furthermore this material has already been shown to maintain viability of cells for over one year,[75] which could prove useful in the fabrication of microarrays as a commercial tool for cell screening. The work described here provides valuable background on the nature of bacterial cells in silica matrices, and is the first work of any kind that investigates the application of sol-gel entrapped cells for compound screening. The

microarray format may be unique in of itself, in contrast to the observations made with bulk monoliths, as the nanolitre volumes of array elements may promote radically different properties and require novel materials to improve cell viability and structural integrity.

Chapter 5 | References

1 Fodor, S.P. *et al.*, Light-directed, spatially addressable parallel chemical synthesis. *Science* 251 (4995), 767-773 (1991).

2 Schena, M., Shalon, D., Davis, R.W., & Brown, P.O., Quantitative monitoring of gene expression patterns with a complementary DNA microarray. *Science* 270 (5235), 467-470 (1995).

3 Lashkari, D.A. *et al.*, Yeast microarrays for genome wide parallel genetic and gene expression analysis. *Proc Natl Acad Sci U S A* 94 (24), 13057-13062 (1997).

4 Schulze, A. & Downward, J., Navigating gene expression using microarrays - a technology review. *Nature Cell Biology* 3 (8), E190-E195 (2001).

5 Espina, V. *et al.*, Protein microarrays: Molecular profiling technologies for clinical specimens. *Proteomics* 3 (11), 2091-2100 (2003).

6 Stoevesandt, O., Taussig, M.J., & He, M.Y., Protein microarrays: high-throughput tools for proteomics. *Expert Review of Proteomics* 6 (2), 145-157 (2009).

7 Narayanaswamy, R. *et al.*, Systematic profiling of cellular phenotypes with spotted cell microarrays reveals mating-pheromone response genes. *Genome Biology* 7 (1), (2006).

8 Nicholson, R.L., Welch, M., Ladlow, M., & Spring, D.R., Small-molecule screening: Advances in microarraying and cell-imaging technologies. *Acs Chemical Biology* 2 (1), 24-30 (2007).

9 Chen, D.S. & Davis, M.M., Molecular and functional analysis using live cell microarrays. *Current Opinion in Chemical Biology* 10 (1), 28-34 (2006).

10 Falsey, J.R., Renil, M., Park, S., Li, S.J., & Lam, K.S., Peptide and small molecule microarray for high throughput cell adhesion and functional assays. *Bioconjugate Chemistry* 12 (3), 346-353 (2001).

11 Schroeder, H., Ellinger, B., Becker, C.F., Waldmann, H., & Niemeyer, C.M., Generation of live-cell microarrays by means of DNA-Directed immobilization of specific cell-surface ligands. *Angew Chem Int Ed Engl* 46 (22), 4180-4183 (2007).

12 Xu, C.W., High-density cell microarrays for parallel functional determinations. *Genome Research* 12 (3), 482-486 (2002).

13 Hook, A.L., Thissen, H., & Voelcker, N.H., Surface manipulation of biomolecules for cell microarray applications. *Trends Biotechnol* 24 (10), 471-477 (2006).

14 Ziauddin, J. & Sabatini, D.M., Microarrays of cells expressing defined cDNAs. *Nature* 411 (6833), 107-110 (2001).

15 Wheeler, D.B., Carpenter, A.E., & Sabatini, D.M., Cell microarrays and RNA interference chip away at gene function. *Nature Genetics* 37, S25-S30 (2005).

16 Palmer, E.L., Miller, A.D., & Freeman, T.C., Identification and characterisation of human apoptosis inducing proteins using cell-based transfection microarrays and expression analysis. *Bmc Genomics* 7, (2006).

[17] Sturzl, M. *et al.*, High throughput screening of gene functions in mammalian cells using reversely transfected cell arrays: Review and protocol. *Combinatorial Chemistry & High Throughput Screening* 11 (2), 159-172 (2008).

[18] Jaluria, P., Betenbaugh, M., Konstantopoulos, K., Frank, B., & Shiloach, J., Application of microarrays to identify and characterize genes involved in attachment dependence in HeLa cells. *Metabolic Engineering* 9 (3), 241-251 (2007).

[19] Mishina, Y.M. *et al.*, Multiplex GPCR assay in reverse transfection cell microarrays. *Journal of Biomolecular Screening* 9 (3), 196-207 (2004).

[20] Fiebitz, A. *et al.*, High-throughput mammalian two-hybrid screening for protein-protein interactions using transfected cell arrays. *Bmc Genomics* 9, (2008).

[21] Conrad, C. *et al.*, Automatic identification of subcellular phenotypes on human cell arrays. *Genome Research* 14 (6), 1130-1136 (2004).

[22] Zhu, Y., Wu, Z.H., Tang, Z.M., & Lu, Z.H., HeLa cell adhesion on various collagen-grafted surfaces. *Journal of Proteome Research* 1 (6), 559-562 (2002).

[23] Hook, A.L., Thissen, H., & Voelcker, N.H., Advanced Substrate Fabrication for Cell Microarrays. *Biomacromolecules* 10 (3), 573-579 (2009).

[24] Chen, Y.C. *et al.*, Lentivirus-mediated RNA interference targeting enhancer of zeste homolog 2 inhibits hepatocellular carcinoma growth through down-regulation of stathmin (vol 46, pg 200, 2007). *Hepatology* 46 (4), 1314-1314 (2007).

[25] Njatawidjaja, E. & Iwata, H., Gene delivery to cells on a miniaturized multiwell plate for high-throughput gene function analysis. *Analytical and Bioanalytical Chemistry* 392 (3), 405-408 (2008).

[26] Sincic, R.S., Chang-Yen, D.A., Eddings, M., Barrows, L.R., & Gale, B.K., Parallel determination of phenotypic cytotoxicity with a micropattern of mutant cell lines. *Biomedical Microdevices* 11 (2), 443-452 (2009).

[27] Scott, C.D., Immobilized Cells - a Review of Recent Literature. *Enzyme and Microbial Technology* 9 (2), 66-73 (1987).

[28] Kourkoutas, Y., Bekatorou, A., Banat, I.M., Marchant, R., & Koutinas, A.A., Immobilization technologies and support materials suitable in alcohol beverages production: a review. *Food Microbiology* 21 (4), 377-397 (2004).

[29] Du, W., Li, W., Sun, T., Chen, X., & Liu, D.H., Perspectives for biotechnological production of biodiesel and impacts. *Applied Microbiology and Biotechnology* 79 (3), 331-337 (2008).

[30] Fesenko, D.O. *et al.*, Alginate gel biochip for real-time monitoring of intracellular processes in bacterial and yeast cells. *Molecular Biology* 39 (1), 84-89 (2005).

[31] Lee, M.Y. *et al.*, Three-dimensional cellular microarray for high-throughput toxicology assays. *Proceedings of the National Academy of Sciences of the United States of America* 105 (1), 59-63 (2008).

[32] Fernandes, T.G., Diogo, M.M., Clark, D.S., Dordick, J.S., & Cabral, J.M.S., High-throughput cellular microarray platforms: applications in drug discovery,

toxicology and stem cell research. *Trends in Biotechnology* 27 (6), 342-349 (2009).

[33] Fernandes, T.G. *et al.*, Three-dimensional cell culture microarray for high-throughput studies of stem cell fate. *Biotechnol Bioeng* 106 (1), 106-118 (2010).

[34] Grant, G.T.M., E. R., Rees, D.A., Smith, P.J.C., & Thom, D., Biological Interactions Between Polysaccharides and Divalent Cations: The Egg-Box Model. *FEBS Letters* 32 (1), 4 (1973).

[35] Bajpai, S.K. & Sharma, S., Investigation of swelling/degradation behaviour of alginate beads crosslinked with Ca^{2+} and Ba^{2+} ions. *Reactive & Functional Polymers* 59 (2), 129-140 (2004).

[36] Sukumaran, S.M., Potsaid, B., Lee, M.Y., Clark, D.S., & Dordick, J.S., Development of a Fluorescence-Based, Ultra High-Throughput Screening Platform for Nanoliter-Scale Cytochrome P450 Microarrays. *Journal of Biomolecular Screening* 14 (6), 668-678 (2009).

[37] Ikeda, Y., Kurokawa, Y., Nakane, K., & Ogata, N., Entrap-immobilization of biocatalysts on cellulose acetate-inorganic composite gel fiber using a gel formation of cellulose acetate-metal (Ti, Zr) alkoxide. *Cellulose* 9 (3-4), 369-379 (2002).

[38] Bottcher, H., Soltmann, U., Mertig, M., & Pompe, W., Biocers: ceramics with incorporated microorganisms for biocatalytic, biosorptive and functional materials development. *Journal of Materials Chemistry* 14 (14), 2176-2188 (2004).

[39] Livage, J. & Coradin, T., Living cells in oxide glasses. *Medical Mineraology and Geochemistry* 64, 315-332 (2006).

[40] Avnir, D., Coradin, T., Lev, O., & Livage, J., Recent bio-applications of sol-gel materials. *Journal of Materials Chemistry* 16 (11), 1013-1030 (2006).

[41] Jin, W. & Brennan, J.D., Properties and applications of proteins encapsulated within sol-gel derived materials. *Analytica Chimica Acta* 461 (1), 1-36 (2002).

[42] Rupcich, N., Goldstein, A., & Brennan, J.D., Optimization of sol-gel formulations and surface treatments for the development of pin-printed protein microarrays. *Chemistry of Materials* 15 (9), 1803-1811 (2003).

[43] Rupcich, N. & Brennan, J.D., Coupled enzyme reaction microarrays based on pin-printing of sol-gel derived biomaterials. *Analytica Chimica Acta* 500 (1-2), 3-12 (2003).

[44] Rupcich, N., Green, J.R.A., & Brennan, J.D., Nanovolume kinase inhibition assay using a sol-gel-derived multicomponent microarray. *Analytical Chemistry* 77 (24), 8013-8019 (2005).

[45] Fennouh, S., Guyon, S., Livage, J., & Roux, C., Sol-gel entrapment of Escherichia coli. *Journal of Sol-Gel Science and Technology* 19 (1-3), 647-649 (2000).

[46] Premkumar, J.R., Rosen, R., Belkin, S., & Lev, O., Sol-gel luminescence biosensors: Encapsulation of recombinant E-coli reporters in thick silicate films. *Analytica Chimica Acta* 462 (1), 11-23 (2002).

[47] Chen, J.B. *et al.*, Efficient immobilization of whole cells of Methylomonas sp strain GYJ3 by sol-gel entrapment. *Journal of Molecular Catalysis B-Enzymatic* 30 (3-4), 167-172 (2004).

[48] Inama, L., Dire, S., Carturan, G., & Cavazza, A., Entrapment of Viable Microorganisms by Sio2 Sol-Gel Layers on Glass Surfaces - Trapping, Catalytic Performance and Immobilization Durability of Saccharomyces-Cerevisiae. *Journal of Biotechnology* 30 (2), 197-210 (1993).

[49] Kuncova, G. *et al.*, Monitoring of the viability of cells immobilized by sol-gel process. *Journal of Sol-Gel Science and Technology* 31 (1-3), 335-342 (2004).

[50] Baca, H.K. *et al.*, Cell-directed assembly of lipid-silica nanostructures providing extended cell viability. *Science* 313 (5785), 337-341 (2006).

[51] Carturan, G., Dellagiacoma, G., Rossi, M., DalMonte, R., & Muraca, M., Encapsulation of viable animal cells for hybrid bioartificial organs by the Biosil method. *Sol-Gel Optics Iv* 3136, 366-373
490 (1997).

[52] Desimone, M.F. *et al.*, Fibroblast encapsulation in hybrid silica-collagen hydrogels. *Journal of Materials Chemistry* 20 (4), 666-668 (2010).

[53] Nguyen-Ngoc, H. & Tran-Minh, C., Sol-gel process for vegetal cell encapsulation. *Materials Science & Engineering C-Biomimetic and Supramolecular Systems* 27 (4), 607-611 (2007).

[54] Carturan, G., Dal Monte, R., Pressi, G., Secondin, S., & Verza, P., Production of valuable drugs from plant cells immobilized by hybrid sol-gel SiO2. *Journal of Sol-Gel Science and Technology* 13 (1-3), 273-276 (1998).

[55] Gautier, C., Livage, J., Coradin, T., & Lopez, P.J., Sol-gel encapsulation extends diatom viability and reveals their silica dissolution capability. *Chem Commun (Camb)* (44), 4611-4613 (2006).

[56] Brook, M.A., Chen, Y., Guo, K., Zhang, Z., & Brennan, J.D., Sugar-modified silanes: precursors for silica monoliths. *Journal of Materials Chemistry* 14 (9), 1469-1479 (2004).

[57] Bhatia, R.B., Brinker, C.J., Gupta, A.K., & Singh, A.K., Aqueous sol-gel process for protein encapsulation. *Chemistry of Materials* 12 (8), 2434-2441 (2000).

[58] Liu, D.M. & Chen, I.W., Encapsulation of protein molecules in transparent porous silica matrices via an aqueous colloidal sol-gel process. *Acta Materialia* 47 (18), 4535-4544 (1999).

[59] Avnir, D., Braun, S., Lev, O., & Ottolenghi, M., Enzymes and Other Proteins Entrapped in Sol-Gel Materials. *Chemistry of Materials* 6 (10), 1605-1614 (1994).

[60] Chen, Y., Zhang, Z., Sui, X.H., Brennan, J.D., & Brook, M.A., Reduced shrinkage of sol-gel derived silicas using sugar-based silsesquioxane precursors. *Journal of Materials Chemistry* 15 (30), 3132-3141 (2005).

[61] Brennan, J.D., Biofriendly sol-gel processing for the entrapment of soluble and membrane-bound proteins: Toward novel solid-phase assays for high-throughput screening. *Accounts of Chemical Research* 40 (9), 827-835 (2007).

62 MacCraith, B.D. & McDonagh, C., Enhanced fluorescence sensing using sol-gel materials. *Journal of Fluorescence* 12 (3-4), 333-342 (2002).

63 Lebert, J.M., Forsberg, E.M., & Brennan, J.D., Solid-phase assays for small molecule screening using sol-gel entrapped proteins. *Biochemistry and Cell Biology-Biochimie Et Biologie Cellulaire* 86 (2), 100-110 (2008).

64 CARTURAN *et al.*, *Inorganic gels for immobilization of biocatalysts: inclusion of invertase-active whole cells of yeast (Saccharomyces cerevisia) into thin layers of SiO[2] gel deposited on glass sheets*. (Elsevier Sequoia, Lausanne, SUISSE, 1989).

65 Sagi, E. *et al.*, Fluorescence and bioluminescence reporter functions in genetically modified bacterial sensor strains. *Sensors and Actuators B-Chemical* 90 (1-3), 2-8 (2003).

66 Pena-Vazquez, E., Maneiro, E., Perez-Conde, C., Moreno-Bondi, M.C., & Costas, E., Microalgae fiber optic biosensors for herbicide monitoring using sol-gel technology. *Biosensors & Bioelectronics* 24 (12), 3538-3543 (2009).

67 Kataoka, K. *et al.*, An organic-inorganic hybrid scaffold for the culture of HepG2 cells in a bioreactor. *Biomaterials* 26 (15), 2509-2516 (2005).

68 Dickson, D.J., Page, C.J., & Ely, R.L., Photobiological hydrogen production from Synechocystis sp PCC 6803 encapsulated in silica sol-gel. *International Journal of Hydrogen Energy* 34 (1), 204-215 (2009).

69 Leonard, A. *et al.*, Cyanobacteria immobilised in porous silica gels: exploring biocompatible synthesis routes for the development of photobioreactors. *Energy & Environmental Science* 3 (3), 370-377 (2010).

70 Carturan, G. *et al.*, Gas-phase silicon alkoxide reactivity vs. Na-alginate droplets for conjugation of alginate and sol-gel technologies. *Journal of Sol-Gel Science and Technology* 37 (1), 69-77 (2006).

71 Carturan, G., Dal Toso, R., Boninsegna, S., & Dal Monte, R., Encapsulation of functional cells by sol-gel silica: actual progress and perspectives for cell therapy. *Journal of Materials Chemistry* 14 (14), 2087-2098 (2004).

72 Boninsegna, S. *et al.*, Encapsulation of individual pancreatic islets by sol-gel SiO2: A novel procedure for perspective cellular grafts. *Journal of Biotechnology* 100 (3), 277-286 (2003).

73 Coiffier, A., Coradin, T., Roux, C., Bouvet, O.M.M., & Livage, J., Sol-gel encapsulation of bacteria: a comparison between alkoxide and aqueous routes. *Journal of Materials Chemistry* 11 (8), 2039-2044 (2001).

74 Premkumar, J.R. *et al.*, Fluorescent bacteria encapsulated in sol-gel derived silicate films. *Chemistry of Materials* 14 (6), 2676-2686 (2002).

75 Alvarez, G.S., Foglia, M.L., Copello, G.J., Desimone, M.F., & Diaz, L.E., Effect of various parameters on viability and growth of bacteria immobilized in sol-gel-derived silica matrices. *Applied Microbiology and Biotechnology* 82 (4), 639-646 (2009).

76 Nassif, N. *et al.*, A sol-gel matrix to preserve the viability of encapsulated bacteria. *Journal of Materials Chemistry* 13 (2), 203-208 (2003).

77 Cho, E.J. & Bright, F.V., Pin-printed chemical sensor arrays for simultaneous multianalyte quantification. *Analytical Chemistry* 74 (6), 1462-1466 (2002).

78 Cho, E.J. *et al.*, Tools to rapidly produce and screen biodegradable polymer and sol-gel-derived xerogel formulations. *Applied Spectroscopy* 56 (11), 1385-1389 (2002).

79 Monton, M.R.N. *et al.*, A Sol-Gel-Derived Acetylcholinesterase Microarray for Nanovolume Small-Molecule Screening. *Analytical Chemistry* 82 (22), 9365-9373 (2010).

80 Zaslaver, A. *et al.*, A comprehensive library of fluorescent transcriptional reporters for Escherichia coli. *Nature Methods* 3 (8), 623-628 (2006).

81 Powers, T. & Noller, H.F., Dominant Lethal Mutations in a Conserved Loop in 16s Ribosomal-RNA. *Proceedings of the National Academy of Sciences of the United States of America* 87 (3), 1042-1046 (1990).

82 Cuny, C., Lesbats, M.N., & Dukan, S., Induction of a global stress response during the first step of Escherichia coli plate growth. *Applied and Environmental Microbiology* 73 (3), 885-889 (2007).

83 Wu, L., Lin, X.M., & Peng, X.X., From proteome to genome for functional characterization of pH-dependent outer membrane proteins in Escherichia coli. *J Proteome Res* 8 (2), 1059-1070 (2009).

84 Han, K.Y., Park, J.S., Seo, H.S., Ahn, K.Y., & Lee, J., Multiple stressor-induced proteome responses of Escherichia coli BL21(DE3). *J Proteome Res* 7 (5), 1891-1903 (2008).

85 Chang, D.E., Smalley, D.J., & Conway, T., Gene expression profiling of Escherichia coli growth transitions: an expanded stringent response model. *Mol Microbiol* 45 (2), 289-306 (2002).

86 Bury-Mone, S. *et al.*, Global Analysis of Extracytoplasmic Stress Signaling in Escherichia coli. *Plos Genetics* 5 (9), (2009).

87 Joseph, T.C., Rajan, L.A., Thampuran, N., & James, R., Functional characterization of trehalose biosynthesis genes from E. coli: an osmolyte involved in stress tolerance. *Mol Biotechnol* 46 (1), 20-25.

88 Barth, M., Marschall, C., Muffler, A., Fischer, D., & Henggearonis, R., Role for the Histone-Like Protein H-Ns in Growth Phase-Dependent and Osmotic Regulation of Sigma(S) and Many Sigma(S)-Dependent Genes in Escherichia-Coli. *Journal of Bacteriology* 177 (12), 3455-3464 (1995).

89 Ferrer, M.L., Garcia-Carvajal, Z.Y., Yuste, L., Rojo, F., & del Monte, F., Bacteria viability in sol-gel materials revisited: Cryo-SEM as a suuitable tool to study the structural integrity of encapsulated bacteria. *Chemistry of Materials* 18 (6), 1458-1463 (2006).

90 Faulkner, W.R., King, J.W., & Chemical Rubber Company., *Manual of clinical laboratory procedures*, [2d ed. (Chemical Rubber Co., Cleveland,, 1970).

[91] Perullini, M., Jobbagy, M., Soler-Illia, G.J.A.A., & Bilmes, S.A., Cell growth at cavities created inside silica monoliths synthesized by sol-gel. *Chemistry of Materials* 17 (15), 3806-3808 (2005).

[92] Burton, E., Yakandawala, N., LoVetri, K., & Madhyastha, M.S., A microplate spectrofluorometric assay for bacterial biofilms. *Journal of Industrial Microbiology & Biotechnology* 34 (1), 1-4 (2007).

[93] Chaudhuri, S., Jana, B., & Basu, T., Why does ethanol induce cellular heat-shock response? *Cell Biology and Toxicology* 22 (1), 29-37 (2006).